



Journal  
of

## Contaminant Hydrology

*Editors*

**E.O. Frind**, Waterloo (Canada)  
**P.L. Bjerg**, Lyngby (Denmark)  
**P. Grathwohl**, Tübingen (Germany)  
**A.J. Valocchi**, Urbana, IL (U.S.A.)

This article was originally published in a journal published by Elsevier, and the attached copy is provided by Elsevier for the author's benefit and for the benefit of the author's institution, for non-commercial research and educational use including without limitation use in instruction at your institution, sending it to specific colleagues that you know, and providing a copy to your institution's administrator.

All other uses, reproduction and distribution, including without limitation commercial reprints, selling or licensing copies or access, or posting on open internet sites, your personal or institution's website or repository, are prohibited. For exceptions, permission may be sought for such use through Elsevier's permissions site at:

<http://www.elsevier.com/locate/permissionusematerial>

# The effect of changes in surface wettability on two-phase saturated flow in horizontal replicas of single natural fractures

Elisa Bergslien<sup>a,\*</sup>, John Fountain<sup>b,1</sup>

<sup>a</sup> *Earth Sciences and Science Education Department, 271 Science Building, Buffalo State College, 1300 Elmwood Ave., Buffalo, NY 14222, USA*

<sup>b</sup> *Department of Marine, Earth and Atmospheric Sciences, Campus Box 8208, North Carolina State University, Raleigh, North Carolina 27695-8208, USA*

Received 2 August 2005; received in revised form 24 May 2006; accepted 17 June 2006

Available online 24 August 2006

---

## Abstract

By using translucent epoxy replicas of natural single fractures, it is possible to optically measure aperture distribution and directly observe NAPL flow. However, detailed characterization of epoxy reveals that it is not a sufficiently good analogue to natural rock for many two-phase flow studies. The surface properties of epoxy, which is hydrophobic, are quite unlike those of natural rock, which is generally assumed to be hydrophilic. Different surface wettabilities result in dramatically different two-phase flow behavior and residual distributions. In hydrophobic replicas, the NAPL flows in well-developed channels, displacing water and filling all of the pore space. In hydrophilic replicas, the invading NAPL is confined to the largest aperture pathways and flow frequently occurs in pulses, with no limited or no stable channel development, resulting in isolated blobs with limited accessible surface area. The pulsing and channel abandonment behaviors described are significantly different from the piston-flow frequently assumed in current modeling practice. In addition, NAPL never achieved total saturation in hydrophilic models, indicating that significantly more than a monolayer of water was bound to the model surface. Despite typically only 60–80% NAPL saturation, there was generally good agreement between theoretically calculated Young–Laplace aperture invasion boundaries and the observed minimum apertures invaded. The key to determining whether surface wettability is negligible, or not, lies in accurate characterization of the contaminant-geologic media system under study. As long

---

\* Corresponding author. Tel.: +1 716 878 3793; fax: +1 716 878 4524.

E-mail address: [bergslet@buffalostate.edu](mailto:bergslet@buffalostate.edu) (E. Bergslien).

<sup>1</sup> Tel.: +1 919 515 3711.

as the triple-point contact angle of the system is low ( $<20^\circ$ ), the assumption of perfect water wettability is not a bad one.

© 2006 Elsevier B.V. All rights reserved.

*Keywords:* Multiphase flow; Non-aqueous phase liquids; NAPL; Fracture flow; Fracture modeling

---

## 1. Introduction

Non-aqueous phase liquids (NAPLs) have long been recognized as persistent sources of groundwater contaminants (Schwille, 1988; Kueper, 1989; Pankow and Cherry, 1998). Characterizing flow NAPL behavior in fractured geologic media is especially problematic as fractures can not only provide both horizontal and vertical conduits for extensive NAPL migration, they also allow NAPL migration to occur in pathways unassociated with local groundwater flow (Reitsma and Kueper, 1994). Good characterization of NAPL flow behavior and residual distribution is integral to successful modeling and remediation. While there are several other complex issues that are of significance, this discussion is confined to non-reactive, two-phase liquid flow in horizontal fractures with no matrix exchange.

Given these parameters, two key properties greatly influence NAPL flow and residual distribution in fractures: the void geometry of the fracture network and the surface wettability of the fracture material. Significant research has gone into establishing the statistical distribution of apertures within fractures (Brown et al., 1986; Hakami and Barton, 1990; Vickers et al., 1992; etc.), but until recently there has been little research into the effects of different surface wettabilities on NAPL flow and residual distribution. The importance of wettability in modeling flow is well understood in the petroleum industry, but has not been as successfully incorporated into environmental studies (Morrow et al., 1986; Morrow, 1990; Jadhunandan and Marrow, 1995; Powers et al., 1996). As experimental data is lacking in this area, many researchers assume “perfect wettability” of rock surfaces with respect to water (i.e. water contact angles of zero) or very low contact angles ( $10^\circ$  or less) when modeling two liquid systems (Pruess and Tsang, 1990; Kueper and McWhorter, 1991; Mendoza, 1992; Steele and Lerner, 2001). In order to directly observe multiphase flow, several researchers have utilized translucent epoxy models, the surface properties of which are usually poorly characterized (Persoff and Pruess, 1993, 1995; Su, 1995; Geller et al., 1996; Brown et al., 1998).

Since there have been only a small number of attempts to reconcile the theoretical wettability of natural rock with the flow behavior observed in the hydrophobic replicas or to determine whether or not these epoxy models are an appropriate analogue to natural fractures with respect to their surface chemical properties, the main objective of this research is to examine the effect of changes in wettability on NAPL flow and distribution in single fractures and to determine under what conditions the epoxy models in common use are useful analogues for multiphase flow in natural fracture systems.

In a previous paper, the surface tension components and parameters of three materials, epoxy, polystyrene and radio-frequency glow discharge (RFGD) plasma-treated polystyrene, were characterized via surface thermodynamic methodology, using direct contact angle measurements of polar and apolar liquids on flat test samples (Bergslien et al., 2004). The commonly used epoxy was determined to have a mildly hydrophobic surface, and polystyrene was found to have a strongly hydrophobic surface. In contrast, RFGD-treated polystyrene has surface tension components and parameters very similar to those of the common geologic materials such as

calcite and muscovite. As pointed out in the previous work, the techniques commonly used to characterize wettability, which most often involve measurement of water contact angles in air, are severely limited in utility and can lead to conflicting interpretations (Dullien, 1992; Geller et al., 1996; Selker and Schroth, 1998). A more fundamental approach involves surface thermodynamic characterization of the materials of interest. An understanding of the changes in surface wettability due to prolonged contact with NAPLs, NAPL mixtures or surface-active agents is also of great significance (Desmond et al., 1994; Powers and Tamplin, 1995; Powers et al., 1996; Lord, 1999).

## 2. Background

In a two-phase system, there is an interface created by the preferential attraction of the molecules located at the interface for molecules of the same type (Adamson, 1990). This force imbalance between the fluids, manifested as the curvature of the interface between the two fluids, is referred to as the interfacial tension ( $\gamma$ ). The liquid on the concave side of the interface is at a greater pressure than the liquid on the convex side of the interface. This pressure difference can be stated (Corey, 1986):

$$\Delta P = \gamma \left[ \frac{1}{r_1} + \frac{1}{r_2} \right], \quad (1)$$

where  $r_1$  and  $r_2$  are the principle radii of curvature at interface.

When a multi-phase system is in contact with a solid surface, one of the fluids will be preferentially attracted to the solid, enabling it to “wet” the surface and decreasing the pressure on that side of the interface (Adamson, 1990). The relative wettabilities of two immiscible liquids to a specific solid surface can be measured via contact angle ( $\theta$ ). Contact angle is always measured at the fluid–fluid–solid triple point through the wetting fluid, which is defined as having a contact angle of less than  $90^\circ$  (often less than  $70^\circ$ ) (Adamson, 1990). Young’s equation describes the relationship between the contact angle at the three-way interface and the interfacial tension between the components:

$$\cos\theta = (\gamma_{ns} - \gamma_{ws}) / \gamma_{nw} \quad (2)$$

where  $\gamma_{ns}$  is the interfacial tension between the NAPL and the solid,  $\gamma_{ws}$  is the interfacial tension between the water and the solid,  $\gamma_{nw}$  is the interfacial tension between the two fluids, and  $\theta$  is the contact angle measured in degrees at the triple point through the wetting fluid. In most cases of geologic interest, though not all, water will be the wetting phase and NAPL will be the non-wetting phase.

The pressure differential across curved liquid interface between NAPL and water is known as the capillary pressure ( $P_c$ ) and is defined as  $P_c = P_{nw} - P_w$ , where  $P_{nw}$  is the pressure of the non-wetting fluid and  $P_w$  is the pressure of the wetting fluid (Bear, 1972). Assuming that NAPL is the non-wetting phase with respect to water and that the system is in hydrostatic equilibrium, then  $P_c = (\rho_{nw} - \rho_w)gh$ , where  $\rho_{nw}$  and  $\rho_w$  are the non-wetting and wetting phase densities, respectively,  $g$  is the acceleration of gravity and  $h$  is the height of the NAPL pool assuming that the top of the pool is at a capillary pressure of zero. In order for a non-wetting NAPL to invade an open fracture saturated with water, the capillary pressure must exceed the entry pressure at some point along the fracture opening.

The lower pressure wetting fluid will coat the surface of the solid occupying the smallest apertures while the non-wetting fluid, which is at a higher pressure, will be isolated inside the

areas of largest aperture. The pressure difference or capillary pressure ( $P_c$ ) can be related to the size of the aperture invaded by the non-wetting via the Young–Laplace equation:

$$P_c = P_{nw} - P_w = n\gamma_{nw} \cos\theta / b \quad (3)$$

where  $n$  is a shape factor that ranges from 2 (for a parallel plate opening) to 4 (for a circular opening), and  $b$  is the aperture (Mercer and Cohen, 1990; Adamson, 1990). Capillary pressure, which is inversely related to aperture size, must be overcome for a non-wetting fluid to invade saturated media. This threshold capillary pressure is generally referred to as the entry pressure.

Entry pressure is a function of the geometry of the opening. For two parallel planer plates, the first principle radius of curvature ( $r_1$ ) is taken normal to the plane of the fracture and is equal to  $b/2\cos\theta$ , where  $b$  is the width of the aperture and  $\theta$  is the fluid/fluid/rock contact angle, and the second radius of curvature ( $r_2$ ) is assumed not to contact the rock surface and is therefore not constrained by a contact angle (NRC, 1996). This results in an entry pressure of:

$$P_E = \frac{2\gamma\cos\theta}{b}. \quad (4)$$

If the opening is better approximated by a circle, then the entry pressure is better represented by (Kueper and McWhorter, 1991):

$$P_E = \frac{4\gamma\cos\theta}{b}. \quad (5)$$

Since fractures are more usually characterized as elongated, semi-parallel planes rather than bundles of tubes, they are usually assumed to be more accurately represented by the first equation (Kueper and McWhorter, 1991). However, more recently, researchers have found that the assumption that the second radius ( $r_2$ ) of curvature is infinite may be invalid and that including the influence of in-plane curvature results in more accurate modeling of the flow process (Glass et al., 2001; Detwiler et al., 2005).

Once the non-wetting phase has successfully invaded an opening, it will continue to migrate through the fracture via the largest available openings (Kueper and McWhorter, 1991). This means that the invading fluid will not invade the entire fracture plane, but only those areas where the entry pressure is overcome. The wetting liquid theoretically will spontaneously displace the non-wetting fluid from the areas of smallest aperture and will most likely exist as a thin film on the solid in the areas of large aperture. Thus, the two phases will distribute themselves throughout the fracture based on the prevailing capillary pressure. This relationship is known as the capillary pressure–saturation function (Reitsma and Kueper, 1994).

A number of researchers have worked to characterize multiphase flow in saturated fractures (Merrill, 1975; Gentier, 1986; Gentier et al., 1989; Pyrak-Nolte et al., 1990; Fourar et al., 1991; Pyrak-Nolte et al., 1992; Fourar, 1992; Fourar et al., 1993; Persoff and Pruess, 1995; Brown et al., 1998). Some of the earliest work was performed by Romm (1966), who observed the flow of kerosene and water between parallel stainless steel plates lined with substances with differing wettabilities. His work originally suggested that each fluid phase flows in its own pathways and does not interfere with the flow of the other phase, i.e. that the relative permeability of each phase is equal to its saturation ( $k_{ri} = S_i$ ); thus, the sum of the relative permeabilities is equal to one ( $k_{rnw} + k_{rw} = 1$ ).

It is now well understood that the presence of two or more fluids within a fracture significantly reduces the permeability of that fracture to each phase (Pruess and Tsang, 1990; Fourar et al., 1993; Persoff and Pruess, 1995). Theoretical analysis and numerical simulations by Pruess and

Tsang (1990) and Pyrak-Nolte et al. (1992) demonstrate that, when capillary forces dominate, significant phase interference occurs in rough-walled fractures (i.e. the sum of the relative permeabilities  $k_{nw}$  and  $k_w$  is significantly less than one). The two fluids block flow paths and interact in such a fashion as to impede the progress of both. For capillary forces to dominate flow, the capillary number ( $N_c$ ) needs to be less than approximately  $10^{-4}$ , with the capillary number defined as:

$$N_c = \frac{v_w \mu_w}{\gamma_{nw} \cos \theta}, \quad (6)$$

where  $v_w$  is the water velocity,  $\mu_w$  is the viscosity of water,  $\gamma_{nw}$  is the interfacial tension between the fluids and  $\theta$  is the contact angle (Mendoza, 1992).

The theoretical work of Pruess and Tsang (1990) conceptualized rough-walled fractures as two-dimensional porous media whose void space was specified spatially. Thus, a network of local, parallel-plate models with correlated lognormal aperture distributions was used to approximate fractures. Simulated capillary pressure and relative transmissivity curves were generated and strong phase interference, with the relative permeabilities summing to much less than one at intermediate saturations, was found. Immobile non-wetting phase saturations of up to 50% occurred. By testing a range of spatial correlations, they found that significant two-phase flow mobility existed only for anisotropic aperture distributions with significantly larger spatial correlations in the direction of flow than in the direction perpendicular to flow.

A limitation of much of the early work discussed, is the use of artificial fractures with unnatural aperture distributions. Fluid flow in fractures is extremely sensitive to aperture size and distribution and the spatial correlation of apertures also becomes very important under two-phase flow conditions. Following the methodology of Gentier (1986) and Gentier et al. (1989), Persoff and Pruess (1995) created transparent epoxy replicas of natural rock fractures cast in silicon molds. They determined the local aperture by measuring light attenuation. Multiphase flow experiments were conducted using nitrogen gas and water, and phase interference was found to be strong, with the relative permeabilities summing to less than 0.1. Artificially high flow velocities were used for the experiments and, because nitrogen gas was used as the non-wetting phase, its compressibility may have affected the results.

Brown et al. (1998) conducted flow experiments in epoxy casts similar to those created by Persoff and Pruess (1995) and also used a light transmittance technique to determine aperture distribution. In this case, the primary objective of the study was to analyze channel development. Once again a gas, room air in this case, was used as the immiscible fluid phase. Their experiments involved flooding an air filled fracture with water and then drying the fracture out by injecting air. Channeling of flow was observed from the submillimeter- to several centimeter-scale and fluid velocity was found to vary by several orders of magnitude, with a maximum of five times the mean velocity.

Laboratory investigations of liquid flow through unsaturated analogue fractures have shown that flow occurs as a series of fingers in narrow channels (Nicholl et al., 1994; Su et al., 1999; Glass et al., 2002). Invasion of initially dry fractures appears to occur as a series of narrow threads along draining channels, called rivulets, that connect to blobs of advancing fluid (Su et al., 2004). These features are apparently gravity driven and have not been observed in fingered flow in horizontal, unsaturated fractures (Su et al., 1999; Geller et al., 2000).

A key aspect of this study, which differentiates it from the work described above, is the ability to alter the surface wettability of the fracture models used. In addition, this research employs an actual DNAPL in the flow experiments. The flow studies described above were performed using air, an inert gas or an LNAPL as the non-wetting fluid because the commonly available DNAPLs are both

toxic and will dissolve the epoxy used to create the transparent models. A series of perfluorocarbons created by 3M have low toxicity, will not damage the polymers used in model creation and have properties similar to common DNAPL contaminants (MSDS sheet, 3M) (Table 1).

### 3. Methods

Samples of unweathered, fractured rock were collected from sections of the Lockport Group, a Silurian age upwardly shallowing depositional carbonate sequence of massive to medium-bedded dolomite with minor amounts of dolomitic limestone and shale, from quarries located in western New York and Canada (Brett et al., 1995). The Lockport Dolomite is a pervasively fractured and is contaminated by NAPLs at numerous sites throughout Niagara Falls and the neighboring regions, including such examples as Love Canal and Hyde Park near Buffalo, New York and Smithville, near Ontario, Canada.

Samples with visible, unopened fractures were cut into rectangles using a diamond blade rock saw before being carefully opened along the fracture plane in the laboratory. Samples that displayed significant weathering were discarded. Fracture types collected consisted of bedding plane fractures, styloliticly controlled fractures, vertical fractures and fractures with secondary mineral infill.

Using a method based on the work described in Persoff and Pruess (1995) and Hakami and Barton (1990), which was in turn based on Gentier (1986), a fracture casting technique was developed for the creation of translucent plastic models of natural fractures. Molds of the rocks were created using degassed Silpack R-2230 two-part silicone rubber, which is specially designed for mold making and small parts casting. It was chosen for use in this study because it can create molds with “precision surface detail up to 1  $\mu\text{m}$ ” (Silpack Inc., 1996). After the silicone cures and following a post cure, the rock is removed from the silicone mold and the mold surface is gently cleaned.

Fracture casts are creating using Stycast 1267 two-part epoxy resin (Robert McKeown Co.). This epoxy is related to the Eccobond 27 epoxy used in several past studies in the literature, which was manufactured by a previous incarnation of the W.R. Grace Company. Prepared epoxy is poured into a mold in stages and then allowed to cure for a minimum of 24 h in a desiccant chamber. Each cast is given a post cure at 150  $^{\circ}\text{C}$  for 1 to 1.5 h to improve rigidity. The casts are then carefully removed from the mold and stored in a desiccant chamber until use.

Surface treatment, if any, would be applied at this stage. If the surface wettability of the model is to be altered, a thin layer of dissolved polystyrene would be spray-coated onto the model using an air gun. The polystyrene (Scientific Polymer Products, Inc.) is prepared by first cleaning the pellets in an ultrasonicated methanol bath for 5 min, dipping the pellets in hexane for 5 to 10 s and then oven drying the pellets for 10 to 15 min at a low temperature. The polystyrene pellets are dissolved in laboratory grade methyl ethyl ketone ( $\text{CH}_3\text{COC}_2\text{H}_5$ ) (MEK) to form a moderately

Table 1

Physical properties of study fluids (bold) and some common DNAPLs (Mercer and Cohen, 1990; Fisher Scientific, 1998)

	Density ( $\text{g}/\text{cm}^3$ )	Solubility (ppm)	Surface tension ( $\text{dyn}/\text{cm}$ )	Absolute viscosity (cP)
Perfluoro-compound FC-75	1.76	11	15	1.408
<i>n</i> -Dodecane	0.75	0.0034	25.35	1.35
Tetrachloroethene (PCE)	1.63	150	32	0.93
Trichloroethene (TCE)	1.46	1100	29.5	0.566
1,1,1-Trichloroethane (TCA)	1.35	757	25	0.91

viscous liquid. The model may then be used as is or subjected to plasma treatment. The exact quantitative thickness of this polystyrene layer on each of the models is not known, but the layer is thin enough that it cannot be detected with the light transmittance technique used to measure aperture distribution.

In this study, each natural fracture was replicated with three different surfaces. The most hydrophobic surface was that created by the untreated polystyrene coating. The plain epoxy surface can be described as an intermediate. Finally, to create a strongly hydrophilic surface the polystyrene-coated models were altered by exposure to radio frequency glow discharge (RFGD) plasma (also referred to as low-temperature plasma), which introduces hydroxyl functionality. Use of a silicone mold does not have an impact on the wettability characteristics of the resultant epoxy model. Samples of epoxy that had not been in contact with silicone had the same surface thermodynamic properties. The surface chemistry of each of these surfaces is described in greater detail in Bergslien et al., 2004.

Several attempts were made to find a method to macroscopically quantify the accuracy of these models, including manual and laser profilometry, and digital topographic analysis, but to this date no satisfactory method of analysis has been found. In the words of Brown et al. (1998) “the final epoxy replicas were checked for quality of reproduction...by hand fitting them to each other and comparing these to the fit of the two original rock surfaces.”

In the final stage of preparation, the epoxy replica is re-assembled to form a model of a natural fracture. The model is sealed along two opposite edges using Evercoat Formula 27 All-Purpose Filler, a two-part waterproof, polyester resin with no shrinkage, to form no-flow boundaries. The remaining sides are turned into source and sink areas using channeled plastic, which allows uniform flow of water into and out of the fracture edges. The channels are created out of strips of Polycast® Acrylic Safety Glazing, by cutting troughs about 3 mm deep using a rotary tool.

In preparation for flow testing, assembled models are initially flooded with CO<sub>2</sub>, which is much more soluble in water than room air, for a minimum of 1 h. The models are then hooked up to a constant head flow apparatus, flooded with clear, distilled water and monitored until fully saturated. The constant head apparatus is supplied with influent by a Masterflex Microprocessor Pump Drive (Cole Parmer Instruments Company). Thus, the inlet and outlet are constant head boundaries and the sealed sides of the model are no-flow boundaries. The outlet of the model is fixed in position, level with the fracture in elevation. Head on the replica is changed by raising or lowering the inlet constant head apparatus.

Once saturated, the models are placed horizontally in a specially designed light box and transmittance pictures are collected, first of the model flooded with clear water, and then of the model flooded with a dyed water standard. The full saturation of the model with the dye standard is confirmed both through evaluation of the digital images collected and by monitoring the effluent using a U-1100 Spectrophotometer (Hitachi) to ensure that the influent and effluent have the same dye concentration. This information is used to determine the aperture distribution of each of the models using a light attenuation method based on the use of calibration curves (Fig. 1). Gravity and buoyancy effects are negated in this study by the use of only horizontal fracture models.

Over a dozen different models were employed during the course of this investigation. The models discussed in this article have attributes as shown in Table 2.

It is well understood that aperture is very sensitive to changes in stress state (Reimus et al., 1993). Because the goal of this study was assessment of these models for visualization studies, no attempt was made to compress the models nor assess changes in aperture distribution under various stress states. As all of the fractures collected for this study were from near the surface, and

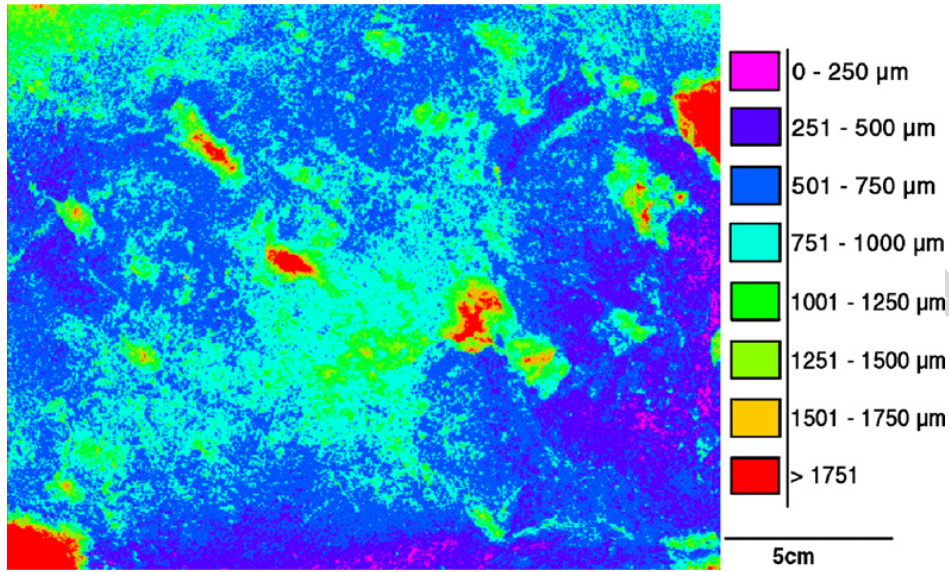


Fig. 1. Optically derived aperture distribution of model RN7-LB.

no additional compression was applied to the resultant models, the apertures are quite large, though not totally out of the ordinary (Shapiro and Nicholas, 1989; Hakami and Barton, 1990; Kumar et al., 1995; Hakami and Larson, 1996). Since the models need to be clear and unblocked for visualization of multi-phase flow, there is no simple way to put them under uniform stress. This constraint needs to be taken into account when evaluating the effectiveness of these models as analogues of in-situ behavior.

Once the model is fully saturated with the dye standard, flow experiments using NAPL can begin. Two NAPLs were used in this study, undyed perfluoro-compound FC-75 ( $C_8F_{16}O$ ), a non-toxic DNAPL analogue for trichloroethene (TCE), one of the most common groundwater contaminants, and dodecane, an LNAPL. The properties of these fluids, along with the properties of some common DNAPL contaminants can be found in Table 1. Clear FC-75 is used for all of the DNAPL experiments allowing the relative saturation to be estimated using the light transmittance techniques discussed previously. Dodecane is used both clear and dyed with Sudan IV, an oil soluble red.

Table 2  
Attributes of models employed in study

Model	Width (cm)	Length (cm)	Fracture type	Approx. volume (ml)	Optical arithmetic mean aperture ( $\mu\text{m}$ ) (S.D.)
RN3	13.6	18.6	Horizontal bedding plane	15.8	470 (443)
RN4	15.9	12.9	Horizontal bedding plane	10	430 (347)
RN7	22.5	19.5	Stylolitically controlled	25+	836 (392)
RN9	~20	18.4	Stylolitically controlled	20	649 (407)
S1	7.7	9.9	Horizontal bedding plane	4.1	417 (201)
SRN31	6.5	18.0	Stylolitically controlled	14	640 (437)

To introduce NAPL into the system, the inlet tubing to the fracture model is closed and the influent for the pump is replaced with NAPL. NAPL is pumped into the constant head flow chamber until it is completely filled. Then the inlet tubing is re-opened and NAPL allowed to fill the tubing. This is meant to mimic conditions in a fracture underlying a NAPL pool. Images of each state of the experiment are collected using a CCD digital camera equipped with narrow bandpass filters. The system is allowed to equilibrate at each state for a minimum of 60 min. The inlet head is incrementally increased by 0.5 cm. The experiment continues until a stable NAPL flow channel is formed.

#### 4. Experimental results

Visual evaluation of the flow experiments demonstrates that surface wettability plays an important role in determining the flow characteristics and the ultimate residual distribution of NAPL. On the strongly hydrophobic untreated polystyrene surfaces, the invasion of NAPL occurs in well-developed channels that flow freely through the model (Fig. 2). Through time, the resident water is almost completely displaced, with few significant zones of residual water remaining (Fig. 2).

NAPL flow in the RFGD plasma-treated hydrophilic models differs substantially. When capillary pressure controls invasion of a non-wetting fluid into the replicas with RFGD plasma-treated surfaces, flow does not initially occur as a continuous stream forming into well-developed channels. Instead invasion occurs as a series of stringers or discrete blobs that are cut into sections by zones of narrow aperture (see Fig. 3). This type of flow involves a series of pulses through the zones of narrow aperture and migration of discrete blobs in the zones of large aperture. Depending on the amount of NAPL invading and the duration of the experiment, channels may or may not eventually develop. In the model shown in Fig. 3, no stable channels ever developed. This flow behavior was initially discovered by Merrill (1975) in his oil and water flow experiments between smooth plates and artificially created fractures, but was dismissed as the product of advective flow between smooth surfaces. The flow experiments in this study indicate that the phenomena Merrill saw could indeed have been the product of capillary flow.

The rough surface of a fracture could cause the creation of discrete blobs through mechanisms similar to the trapping effects cited by Wilson and Conrad (1984) in porous media: by-passing and snap-off. By-passing occurs in porous media when a void is split into two tubes of dissimilar radius by a grain and then rejoined past the obstacle. When, in such a situation, water is forcing out a NAPL, the water will invade through one of the tubes, flushing the NAPL out and reaching the point where the two tubes rejoin into one. This isolates the NAPL in the other tube (Fig. 4). Snap-off occurs in pores with high aspect ratio, where the pore throats are much smaller than the pore bodies. The re-invading water flows along the hydrophilic grain surfaces, displacing the NAPL from the small diameter void spaces and isolating it in the center of the largest void spaces (Fig. 5). Though these mechanisms describe the manner in which NAPL residual blobs are formed during water flushing of porous media, similar mechanisms appear to affect the behavior of NAPL as it invades hydrophilic fractures.

A form of by-passing seems to occur when small embryonic NAPL channels are abandoned after the development of successful, complete NAPL channel (Fig. 6). These areas in the fracture are by-passed when the pressure distribution in the fracture changes in response to the development of the new channel. A variant of snap-off may occur when the small blobs or stringers of NAPL force their way through zones of narrow aperture and are then cut off as water, the wetting fluid, reclaims the small apertures, leaving the NAPL as an isolated blob in a large aperture zone.

If there is a sufficiently large supply of NAPL, a sufficiently long time span, or a sufficiently narrow zone in the fracture that stalls flow for long periods of time, stable flow channels will

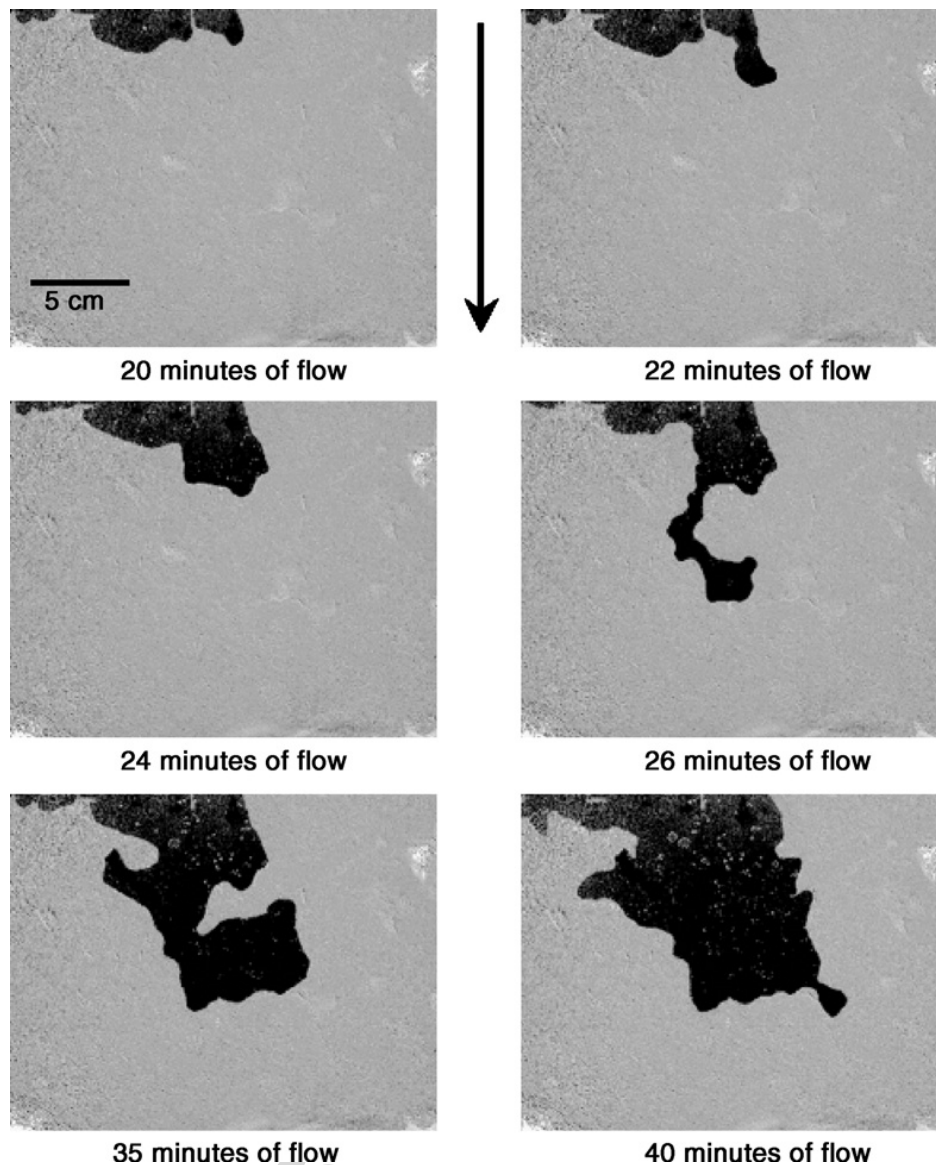


Fig. 2. Injection of FC-75 (dark) into Untreated Polystyrene Surface Fracture Model RN7 which was initially saturated with blue dyed water. Flow occurs from top to bottom at a 3 cm head difference. These results illustrate smooth channel development.

form. When this occurs, the NAPL in other areas of the fracture that fail to form successful channels is abandoned and will usually remain isolated and immobile. Once a stable channel is formed, increases in the pressure of the non-wetting fluid will cause an increase in the size of the channel, i.e. invasion of previously water-filled areas of slightly lower aperture, but unless the widened channel encounters abandoned or isolated NAPL blobs, the increased pressure head does not usually remobilize them (Fig. 7). In addition, some areas of the channel may also be re-invaded by water. The new channel arrangement changes the pressure distribution in the fracture sufficiently that some areas where capillary pressure overcame entry pressure are suddenly dropped below the necessary entry pressure and are spontaneously re-invaded by water (Fig. 7, bottom image).

If there are zones of narrow aperture in the flow channel, flow will occur in pulses (Fig. 8). There are at least two potential explanations for this behavior. The NAPL may be stalled until a continuous path back towards the inlet is formed, with sufficiently high pressure to overcome the

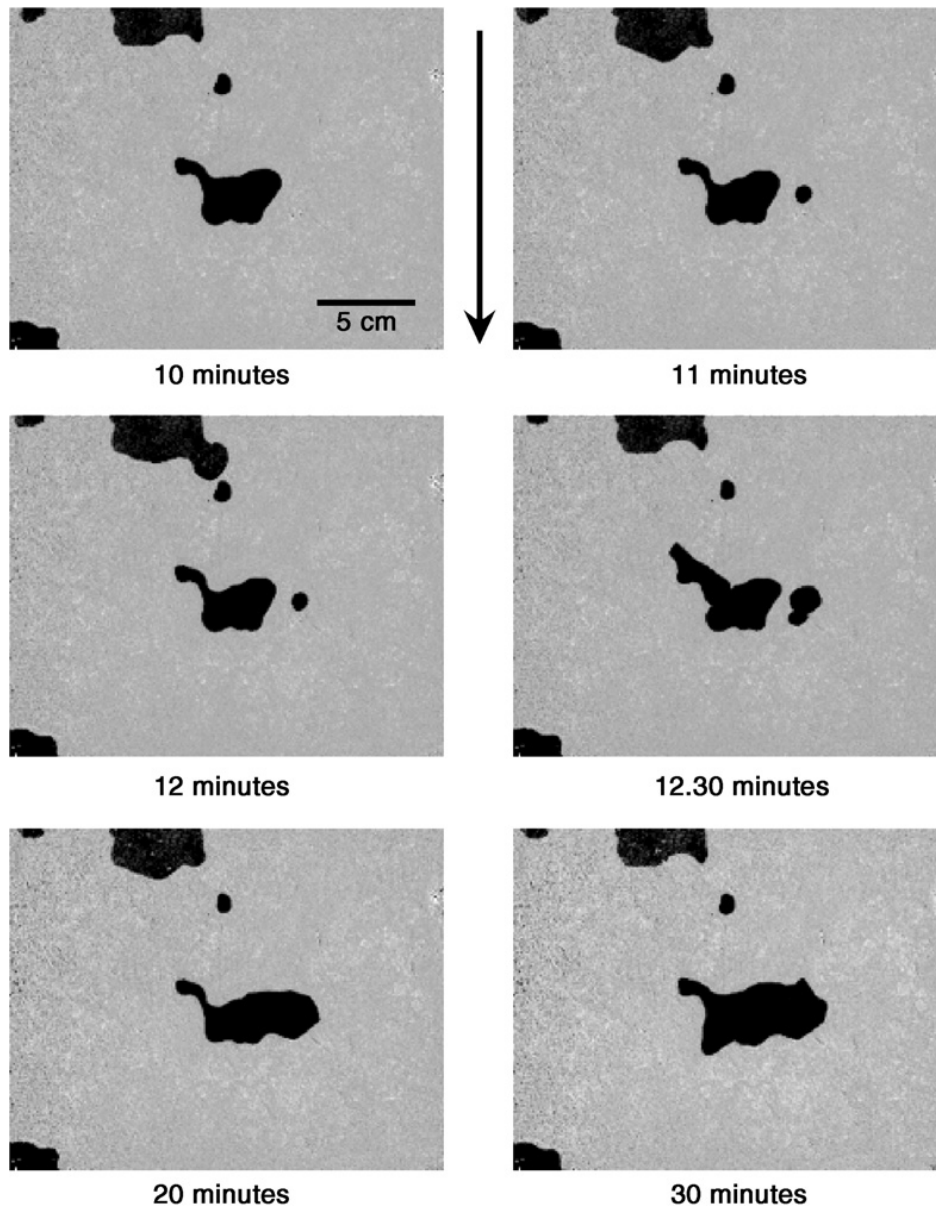


Fig. 3. Injection of FC-75 (dark) into Fracture Model RN7 with polystyrene surface exposed to RFGD plasma for 5 min. Model was originally saturated with dyed water. The inlet head difference is 4 cm and flow is from top to bottom. This experiment illustrates flow with no stable channel development.

entry pressure of the narrow zone. Once the entry pressure is overcome, NAPL flows so quickly into the large aperture area, beyond the constriction, that the tail snaps off. The NAPL that passes through the narrow aperture will either migrate as a blob, or will join into the next section of NAPL filled channel. Because the NAPL blob has been bisected, pressure behind it will be reduced and NAPL flow will stall until once again sufficient pressure is built up to overcome entry pressure.

Another method by which NAPL migrates in pulses is through aging of the fluid interface. The longer the two fluids are in contact, the more dissolution occurs, even with the so-called



Fig. 4. By-passing of the lower channel. Adapted from Wilson and Conrad (1984).

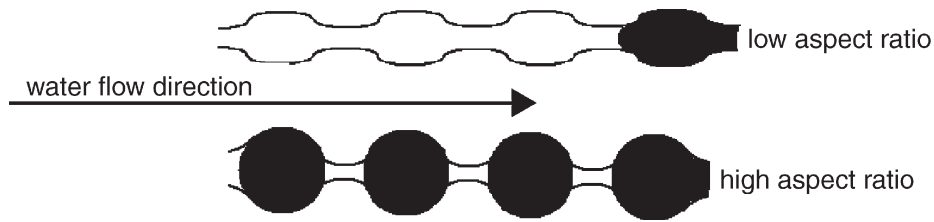


Fig. 5. Snap-off. Adapted from Wilson and Conrad (1984).

immiscible contaminants. This causes the interfacial tension between the fluids to decrease. In a flowing system, the invading NAPL may be stalled long enough for the interfacial tension to drop slightly, allowing the “aged” fluid to continue to migrate. A fresh supply of NAPL reaches the channel neck and is again stalled until the interface ages. Most likely a combination of these two effects, physical snapping of the NAPL blob and interfacial tension drop, causes the pulsing flow behavior seen in the flow experiments, though the flow mechanism is most likely dominant. Thus, there is clear evidence that capillary flow mechanisms exist which can and do cause migration of isolated NAPL blobs through hydrophilic fractures.

The behavior of invading wetting fluids into fracture models saturated with non-wetting fluid and with small average hydraulic aperture ( $<200\ \mu\text{m}$ ) is somewhat different from both of the behaviors described above. In models with larger average hydraulic aperture ( $250\ \mu\text{m}$  or more), the wetting fluid easily displaces the non-wetting fluid and with only a very low fluid pressure gradient can eventually displace the non-wetting fluid fully. However, in models of small average hydraulic aperture ( $<200\ \mu\text{m}$ ), capillary forces act as an instant barrier to flow, i.e. the wetting fluid does not spontaneously displace the non-wetting water in the hydrophobic models (Fig. 9).

Once this capillary barrier is overcome, the wetting fluid will flow freely and eventually displace the non-wetting fluid, but the flow behavior is different from that found in the larger models. The majority of the invading wetting liquid still forms continuous channels, but now there are also isolated blobs of the invading liquid as well. Also, although none of the channels

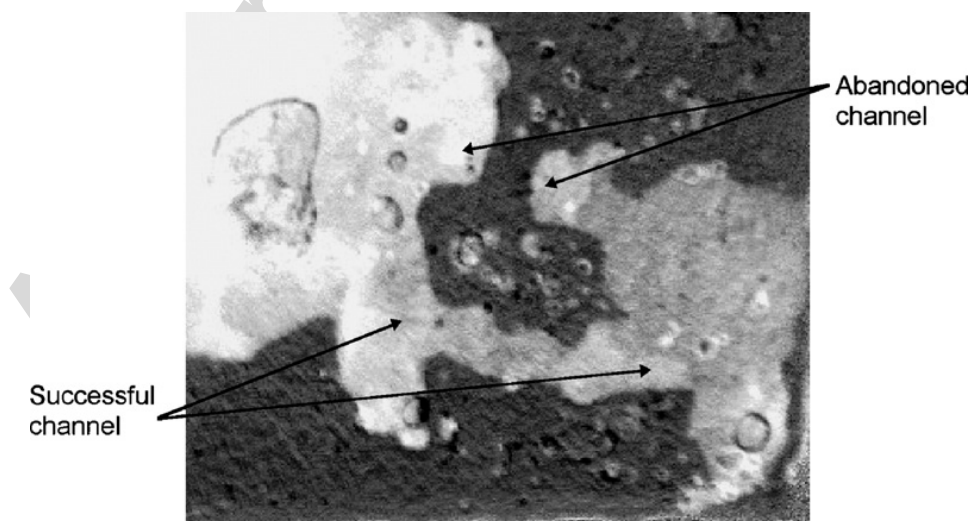


Fig. 6. Channel abandonment in a water saturated hydrophilic fracture replica. The lighter liquid is FC-75 invading from the right and flowing to the left.

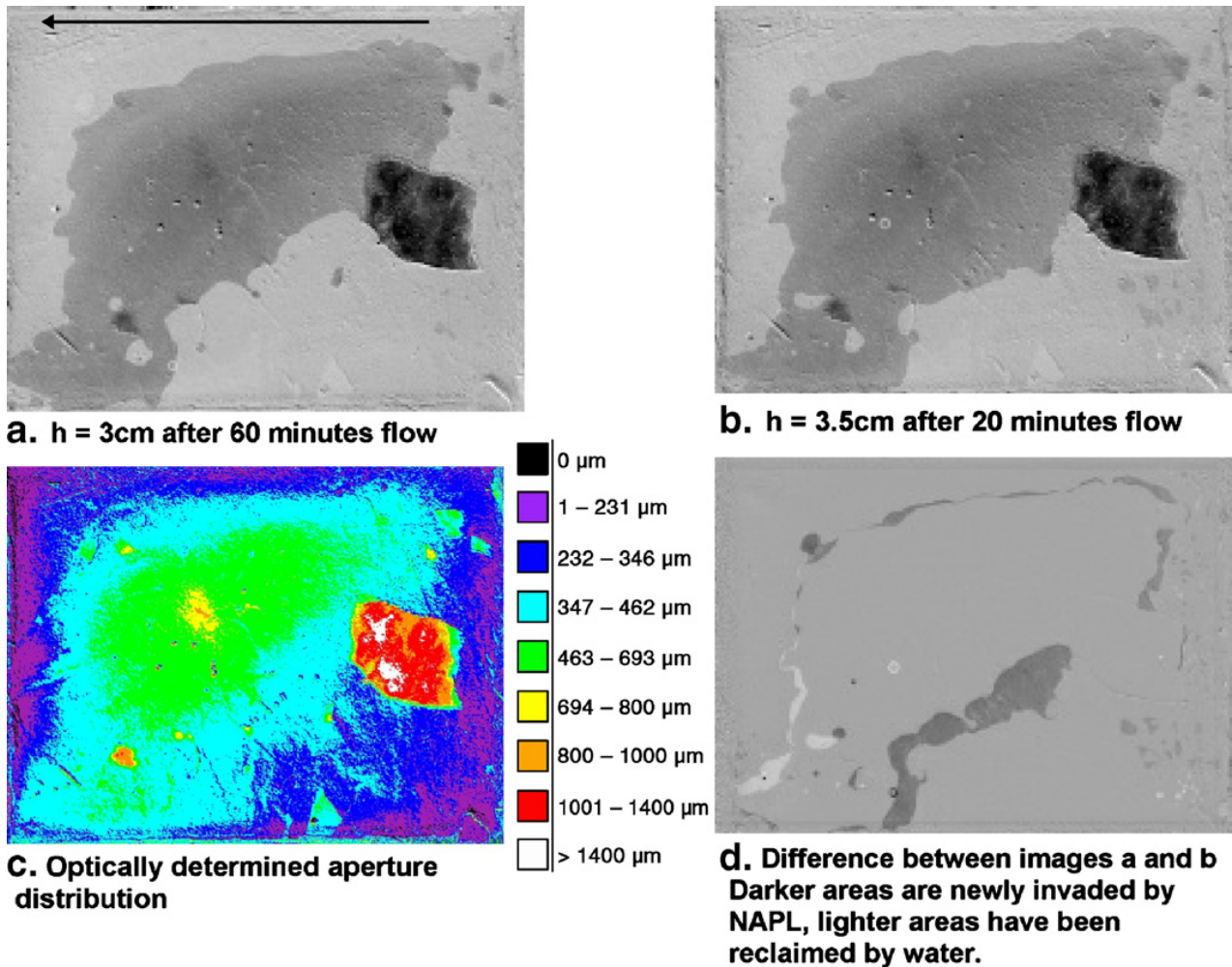


Fig. 7. Images showing full channel development by FC-75 (dark liquid) in RFGD-treated polystyrene-coated fracture model S1 initially saturated with dyed water. Flow is from right to left; the top and bottom are no-flow boundaries. The darker areas in the top two images are the areas invaded by FC-75; the darker the area is the larger the aperture.

formed by the invading wetting fluid are cut-off and abandoned, as occurs when non-wetting NAPL invades a hydrophilic fracture, the channels that do form are narrower and very irregular in shape (Fig. 9). This results in the isolation and entrapment of a significant amount of residual non-wetting fluid. The invading wetting fluid initially displaces the non-wetting fluid from the areas of smallest aperture, resulting in extremely slow flow (on the order of  $<1$  ml/h). Often the channels that are developed in this fashion will surround areas of high aperture, isolating them. Successful displacement of the non-wetting fluid requires a significant increase in wetting fluid pressure.

To ensure that the invasion flow behavior described above was not an artifact of some type of interaction between the perfluoro-compound FC-75 and the tubing and plastic inlet and outlet channels, the same experiment was performed in a RFGD plasma-treated fracture replica of model S1 that was initially saturated with FC-75 and was invaded by water (Fig. 10). Here the wetting fluid (water—the light colored areas) is clearly initially confined to the zones of smallest aperture (Fig. 10). As the pressure head on the water increases, more and more of the FC-75 (the darker areas of the pictures) is forced out of the fracture or is confined to the zones of largest aperture. As water channels are created in new areas, the trapped FC-75 is broken into smaller and smaller isolated blobs. However, even a dramatic increase in head (55 cm head difference) does

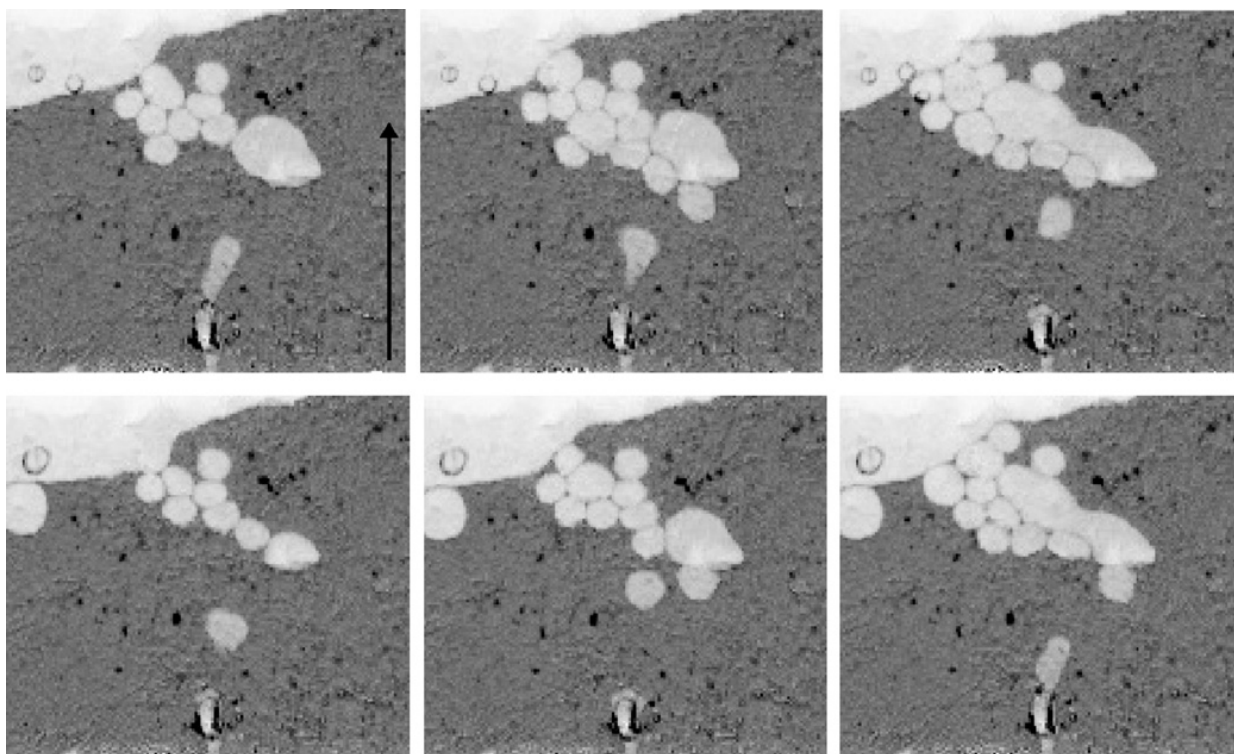


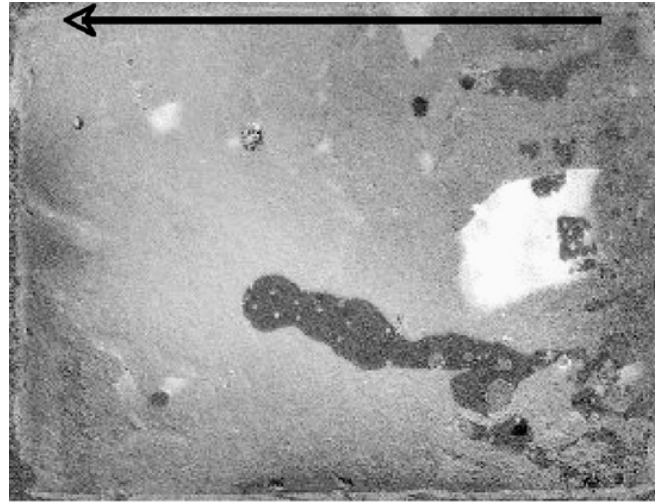
Fig. 8. DNAPL blob migration through RFGD plasma-treated model RN4 initially saturated with 50% Liquitint Blue dyed water standard. Bottom right hand corner, approximately  $4\text{ cm} \times 4\text{ cm}$ , of model. The pictures are  $\sim 15\text{ s}$  apart. Flow is from the bottom to the top.

not result in complete removal of the NAPL. This is unlike the behavior found when FC-75 is the wetting fluid invading a hydrophobic fracture, where complete displacement at much smaller head differences (3–4 cm in the model shown in Fig. 9) is possible.

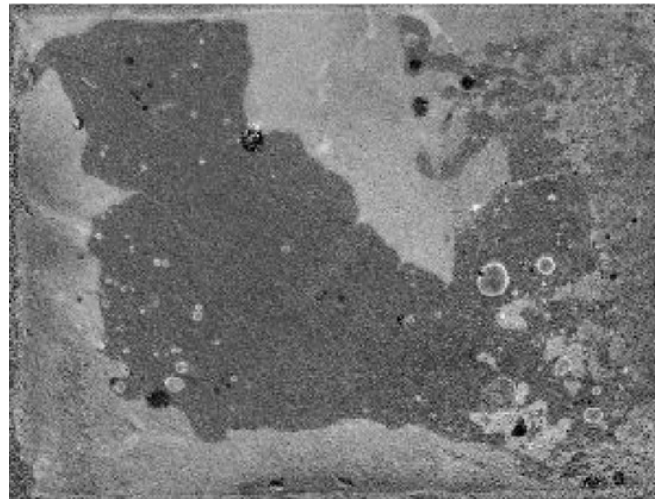
The most likely explanation for the differing flow behaviors of the invading wetting fluids, first FC-75 into a hydrophobic replica, second water into a hydrophilic replica, lies in the initial state of the system. When the model is initially saturated with water, the surface of the model is contaminated by this contact, changing the surface chemistry, and wettability, of that surface. The same kind of contamination occurs when the model is initially saturated with FC-75. These experimental results raise two important points. First, the initial state of the system has a significant effect on the resulting flow behavior. This means that experimentally modeling two-phase flow with alternate fluids and attempting to extrapolate behavior is possibly a futile exercise. Second, prolonged contact between a contaminant and a rock surface will significantly alter that surface. How well the behavior of a fresh laboratory system will compare to the behavior of a natural system that has been in place for months, years or even decades, is questionable and requires further investigation.

## 5. Quantitative findings

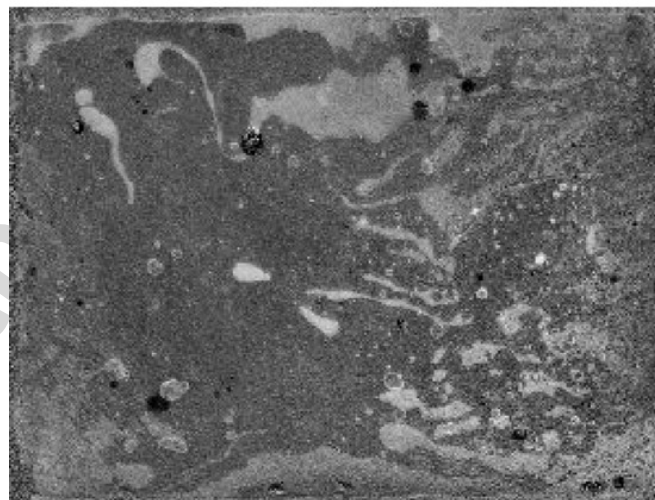
Use of transparent epoxy models allows direct visual determination of the relative saturation of the model by the immiscible fluids migrating through it and allows direct determination of the minimum aperture size invaded by the non-wetting fluids. Relative saturation is determined using basic image math in ENVI (formerly Research Systems, Inc., now ITT Visual Information Solutions). A transmittance image of the model invaded by a clear NAPL is created by dividing



**1 centimeter head difference 36 minutes**



**2 centimeter head difference 10 minutes**



**2 centimeter head difference 27 minutes**

Fig. 9. Invasion of untreated hydrophobic fracture replica S1 by FC-75. The fracture was saturated with blue dyed water. Flow is from right to left. The darker areas are those invaded by FC-75 and the lighter areas are water.

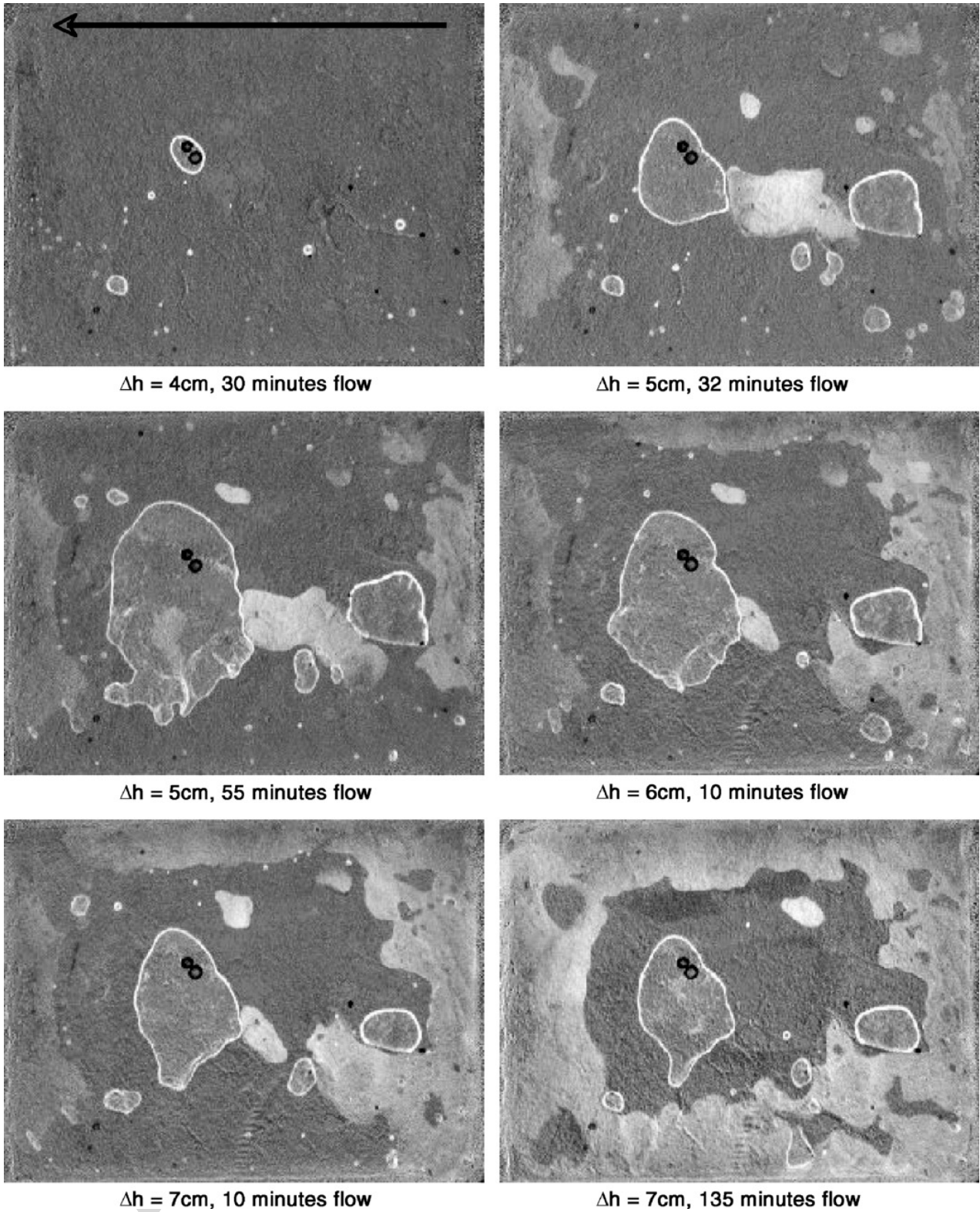


Fig. 10. Dyed water invasion of a RFGD plasma-treated polystyrene-coated fracture replica of fracture S1 initially saturated with FC-75. Flow is from right to left; the top and bottom are no-flow boundaries. The dark fluid is FC-75; water is light colored. Dyed water invasion of a RFGD plasma-treated polystyrene-coated fracture replica of fracture S1 initially saturated with FC-75. Flow is from right to left; the top and bottom are no-flow boundaries. The dark fluid is FC-75; water is light.

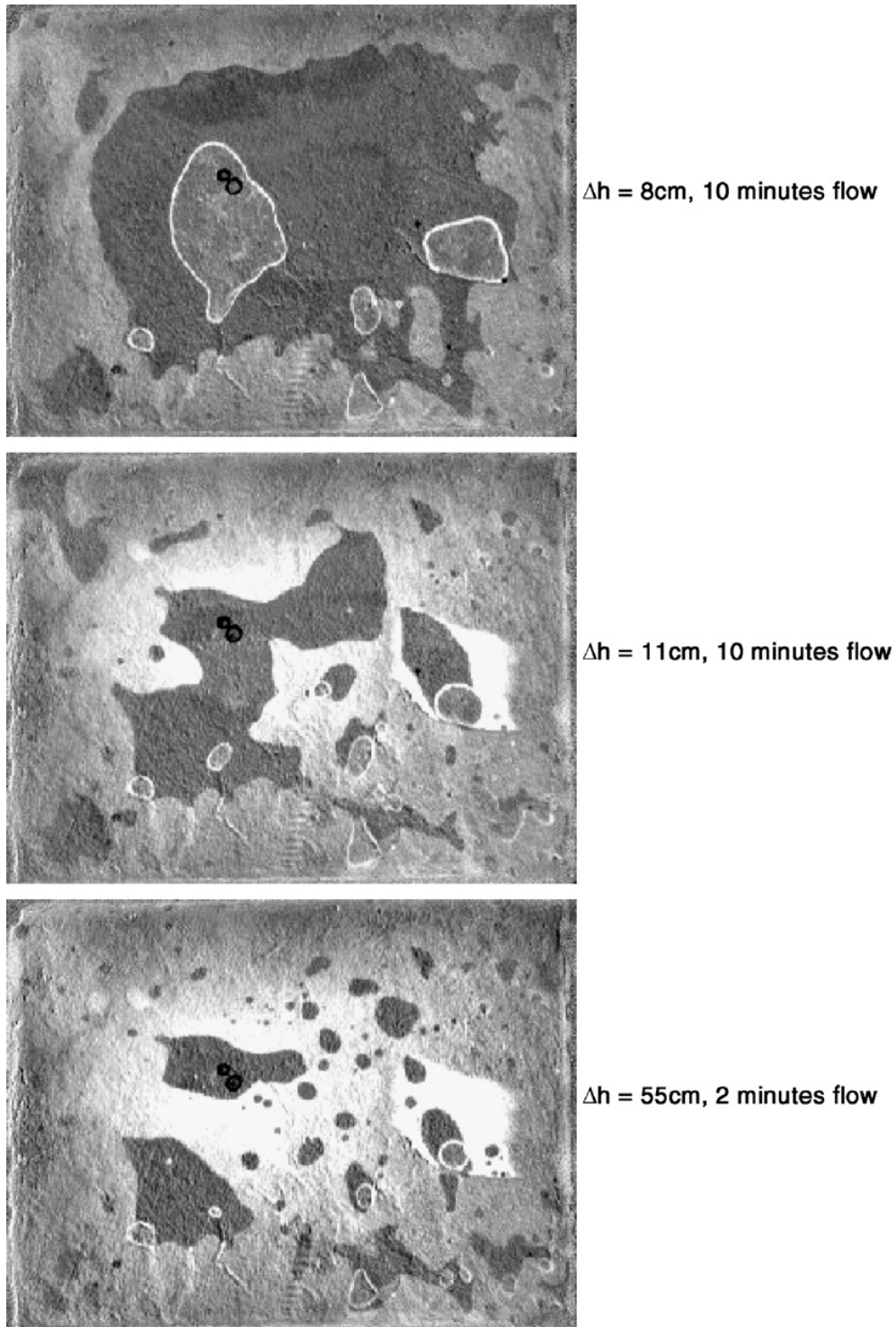


Fig. 10 (continued).

the experimental image by an image of the model flooded with water in NIH Image (NIH). The transmittance image is then converted into an “apertures still invaded by water” image using the same light transmittance method used to determine aperture distribution. Relative saturation is calculated by dividing the “apertures still invaded” image by a full aperture distribution image and multiplied by 100. The result is an image with values from 0 to 100 representing percent saturation by water (Fig. 11).

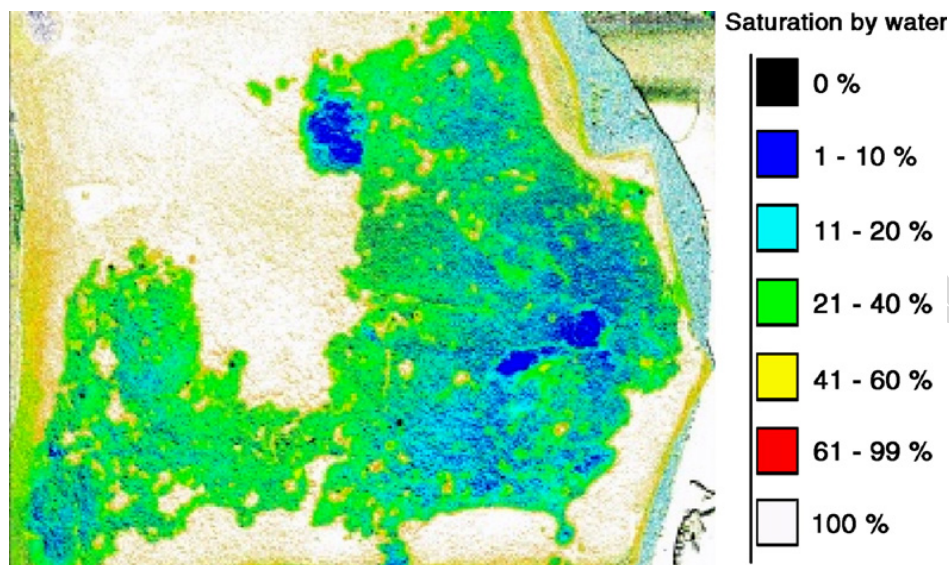


Fig. 11. Percent saturation of water in RFGD plasma-treated fracture replica RN9 invaded by FC-75. White areas are completely saturated by water. There are no areas in the model 100% occupied by FC-75.

In all of the hydrophilic fracture replicas invaded by FC-75, the invading non-wetting fluid does not achieve full saturation in any part of the model. The maximum saturation achieved by the invading non-wetting fluid is a little over 90% in the areas of maximum aperture, more commonly it ranges between 60% and 80%. The fact that there is significantly more than a monolayer of water lining the walls of the replica is a surprise. These findings suggest that the non-wetting invasive fluid could be migrating through the center of the fracture void space, while the wetting fluid thickly coats the top and bottom solid surfaces. If this is indeed the case, it brings into question the validity of the Young–Laplace equation in interpreting two-phase flow, since the invading liquid is not in contact with the solid surface. Immobile water also pools around asperities and becomes trapped in surface irregularities, but these mechanisms could only account for a very small portion of the water detected.

It is also possible that the two fluids become layered, with the denser FC-75 underlying a thick layer of water (Fig. 12). The significantly higher density of FC-75 ( $1.76 \text{ g/cm}^3$ ) and the extraordinarily strong bonds formed within water make this a distinct possibility. In this case, some version of the Young–Laplace equation would still apply. Additional work, with a radically modified experimental apparatus, is required to determine if any one of these theories is correct or if some other mechanism is responsible. It is also worth noting that the

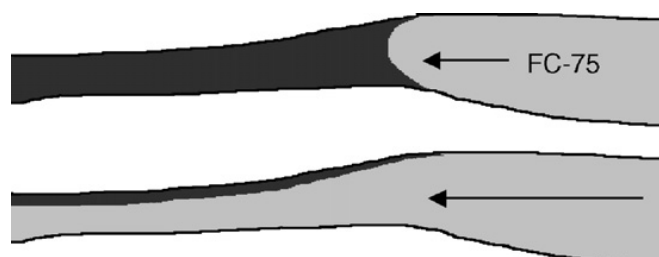


Fig. 12. Layering of Invading FC-75 (lighter liquid).

maximum saturation value reached in the invaded areas with well-developed channels does not change significantly as the non-wetting fluid pressure increases.

These relative saturation images lead to the tentative suggestion that a change in the theories concerning the manner in which two-phase flow occurs may be in order. The invasion of a NAPL is usually theorized to occur as piston-flow, where apertures switch from one hundred percent occupation by water to one hundred percent occupation by the invading NAPL once critical entry pressure is achieved (Kueper and McWhorter, 1991; Mendoza, 1992). It is clear from this study that the invading NAPL does not completely displace the resident water and that the actual saturation is not linearly related to aperture size. Currently, the transmissivity of a cell, or area of distinct aperture, within a fracture is assumed to be zero if it is not completely occupied by a single fluid phase (Pruess and Tsang, 1990; Mendoza, 1992). The results of this study demonstrate that the invading NAPL successfully forms flow channels with significantly less than 100% NAPL occupation. Rather than piston-flow, where one fluid completely displaces another resulting in 100% occupation, it appears that something else is happening. The results presented here are only preliminary and represent an avenue for future work.

The observed minimum aperture invaded in each of the replicas was compared to the theoretical minimum aperture invaded, calculated using the Young–Laplace equation, in order to shed some light on whether or not the equation is useful or even applicable. The approximate minimum aperture invaded in each of the models is determined using ENVI's masking and region of interest (ROI) functions. First a masking image is generated by dividing an image of the fracture flooded with clear FC-75 by an image of the fracture saturated by dyed water multiplied by one hundred. This creates an image where areas flooded by water have a value of 100 and areas flooded with FC-75 will have values greater than 100. This image is turned into a mask where anything with a value of 100 or less is blacked out. The mask is overlain upon an aperture distribution image of the fracture (Fig. 13). The ROI function is used to select the very edge of the invaded area and the statistics function is used to get the range of values invaded at the border. Because the pressure distribution changes when there is flow within the model, only images where the invading fluid is stationary and at equilibrium are used for this calculation. This minimum aperture invaded can then be compared to the theoretical aperture invaded as calculated by the Young–Laplace Eq. (3) (Fig. 14).

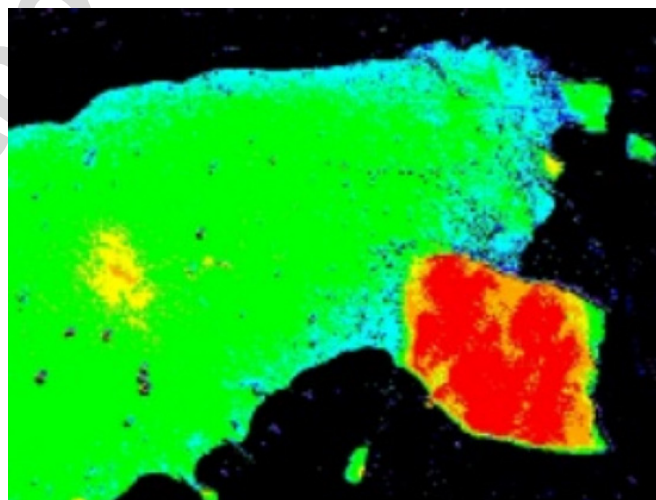


Fig. 13. Upper right quadrant of fracture replica S1 with mask applied.

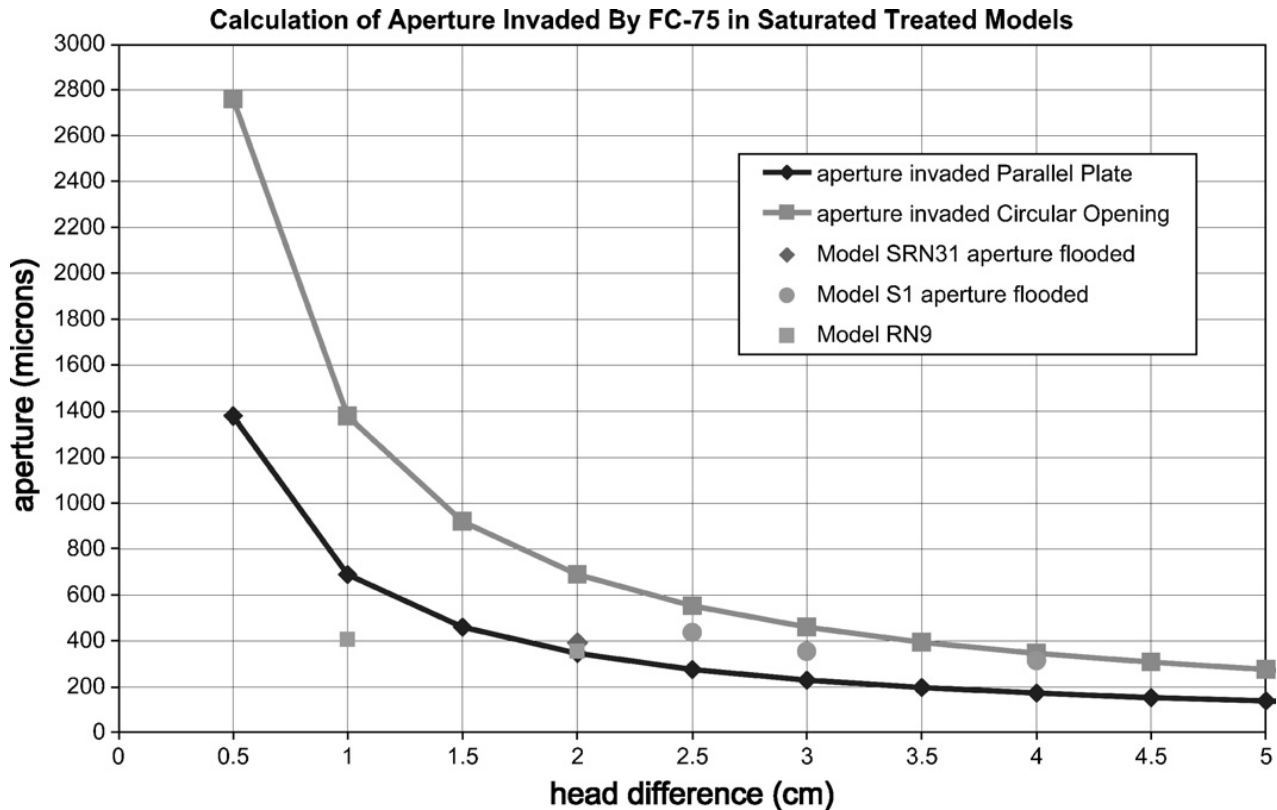


Fig. 14. Actual and theoretical minimum aperture invaded by FC-75 in RFGD-treated models initially saturated with water triple-point contact angle =  $14.4^\circ$ .

In Fig. 14, the upper line represents the theoretical minimum circular aperture invaded by perfluoro-compound FC-75 as calculated using the Young–Laplace equation, while the lower line represents the theoretical minimum parallel plate aperture invaded. Thus, these lines demarcate the theoretical limits of the range of minimum aperture invaded. Results for three of the models, with RFGD-treated surfaces and triple-point contact angles of  $\sim 14.4^\circ$  (RN9, S1 and SRN31), are compared to these theoretical boundaries in Fig. 14. Models S1 and SRN31 fall neatly within these boundaries; thus, for these two models, there is good agreement between the predicted entry pressure and the observed entry pressure.

The third model, RN9, falls below the lower boundary at a head difference of 1 cm, indicating that significantly smaller apertures were invaded than predicted by the Young–Laplace equation. This behavior is more like that of a model with a substantially higher triple-point contact angle. For a triple-point contact angle of  $14^\circ$ , the predicted minimum parallel plate aperture invaded is  $690 \mu\text{m}$ , while for a contact angle of  $48^\circ$  the predicted aperture invaded is  $468 \mu\text{m}$ . Due to the size and roughness of the model, and the nature of the plasma treatment, which varies slightly with distance from the source, it is entirely possible that one end or one section of this model did not receive sufficient exposure to the RFGD plasma. If this was indeed the case, then in the future more care should be taken with the placement of the models in the plasma chamber and a more detailed examination of the surface performed prior to use.

The other possibility is that the area of the model where the observed minimum aperture invaded was determined is extremely rough. Surface roughness increases contact angle and, if there is an area in the model of significantly higher surface roughness, this could account for the invasion of areas of smaller than predicted aperture. At 2 cm of head difference, the observed and predicted behaviors were once again in good agreement for this model. A constant head apparatus

capable of accurately achieving head differences of less than 1 cm would also be useful for further analysis of this behavior.

A similar comparison of theoretical minimum aperture invaded and observed aperture invaded can be seen in Fig. 15. Here the models have RFGD plasma-treated surfaces with triple-point contact angles of  $\sim 48^\circ$ . In this case, one of the models, RN4LB, appears to have very good agreement between the predicted and observed entry. In the other model, S1-T2, the observed minimum aperture invaded is much larger than predicted, until a head difference of 4 cm is achieved. In this case, there is a zone of large aperture in the model that is not filled until the pressure is increased sufficiently that a large supply of NAPL is able to flow through the low aperture zone at the inlet. Initially, there are no smaller apertures available for invasion.

Based on the generally good agreement between the theoretically calculated aperture invasion boundaries and the observed minimum apertures invaded, it appears that the Young–Laplace equation is, in fact, useful and valid. If there were no contact between the invading FC-75 and the replica walls, there should be no difference between the invasion behaviors for hydrophilic models of different quantitative wettability. Instead, differences in absolute hydrophilic wettability do result in different minimum observed apertures invaded. The fact that the areas of largest aperture have the highest NAPL saturation, and that the total saturation of the fracture by the invading NAPL increases as capillary pressure increases, also support the assertion that the Young–Laplace equation is valid.

Contact angle hysteresis, the difference between advancing and retreating contact angles, can have a significant effect on flow behavior (Dullien, 1992; Su et al., 2004). Some researchers have

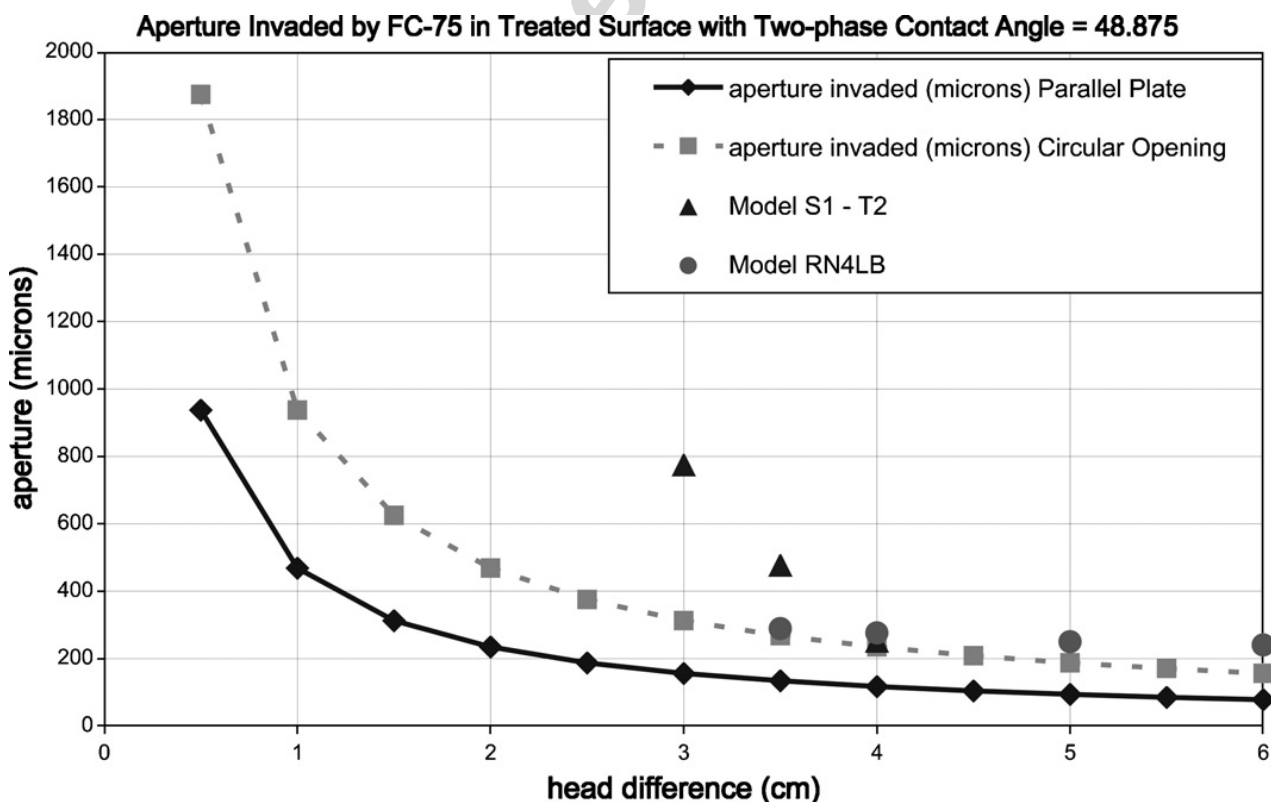


Fig. 15. Actual and theoretical minimum aperture invaded by FC-75 in RFGD-treated models initially saturated with water triple-point contact angle =  $48^\circ$ .

measured differences of greater than  $20^\circ$  (Laroussi and DeBacker, 1979; Bradford and Leij, 1995). This effect is most pronounced in non-horizontal, unsaturated systems, where the invading liquid is displacing air (Su et al., 2004). An advancing liquid will virtually always be wetting in comparison to air. Advancing contact angles are always greater than retreating contact angles, due primarily to contamination of the surface. This would imply that contact angle between the non-wetting fluid and the fracture model surface will alter after first contact, and through time as the chemistry of the solid surface alters (Powers et al., 1996; Bergslien et al., 2004). Theoretically, the pathways followed through a model by non-wetting NAPL should become a zone of altered surface chemistry, which through time could turn these pathways into hydrophobic conduits for flow.

Over the course of the experiments described in this article, no consistent, measurable change in contact angle was detected during flow. Contact angle hysteresis associated with the initial invasion of the non-wetting fluid may be too subtle for the experimental set-up to detect. On the other hand, the fact that NAPL did not achieve total saturation of any of the models indicates that at least some of the fracture surfaces have water coatings that provide a buffer to surface contamination. None of the flow experiments described here lasted more than a few weeks so the potential development of pathways due to long-term alteration of surface chemistry was not tested. It is possible that contact angle hysteresis over the short term is not as significant an effect in liquid–liquid systems.

Examination of the aperture invasion curves for perfluoro-compound FC-75 (Fig. 16) and dodecane (Fig. 17) reveals that the behavior of the epoxy is significantly different from the behavior of both the treated polystyrene surface, which was shown to be a good analogue for Lockport Dolomite, and from the behavior of a water-wet surface, the theoretical analogue used for silica minerals. This is especially apparent in the flow behavior of dodecane into an epoxy

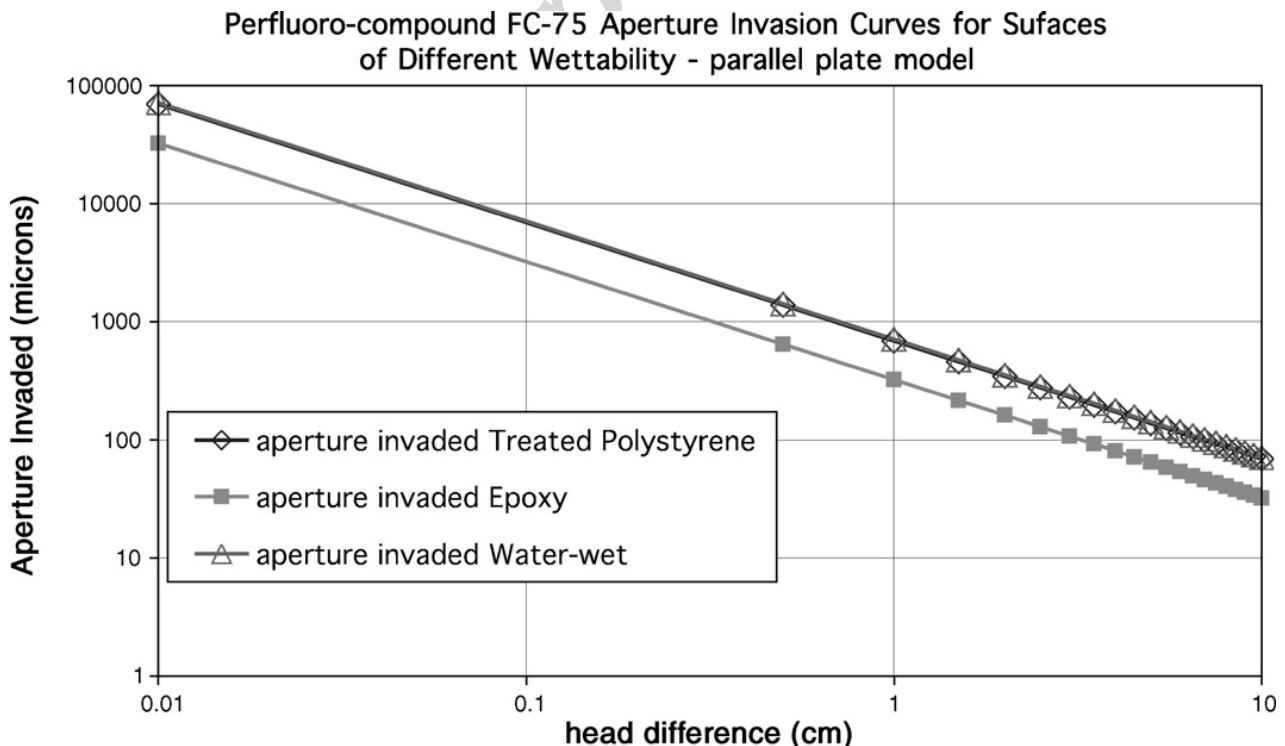


Fig. 16. Perfluoro-compound invasion curves for surfaces of differing wettability. The lines for water-wet and treated polystyrene are almost overlapping.

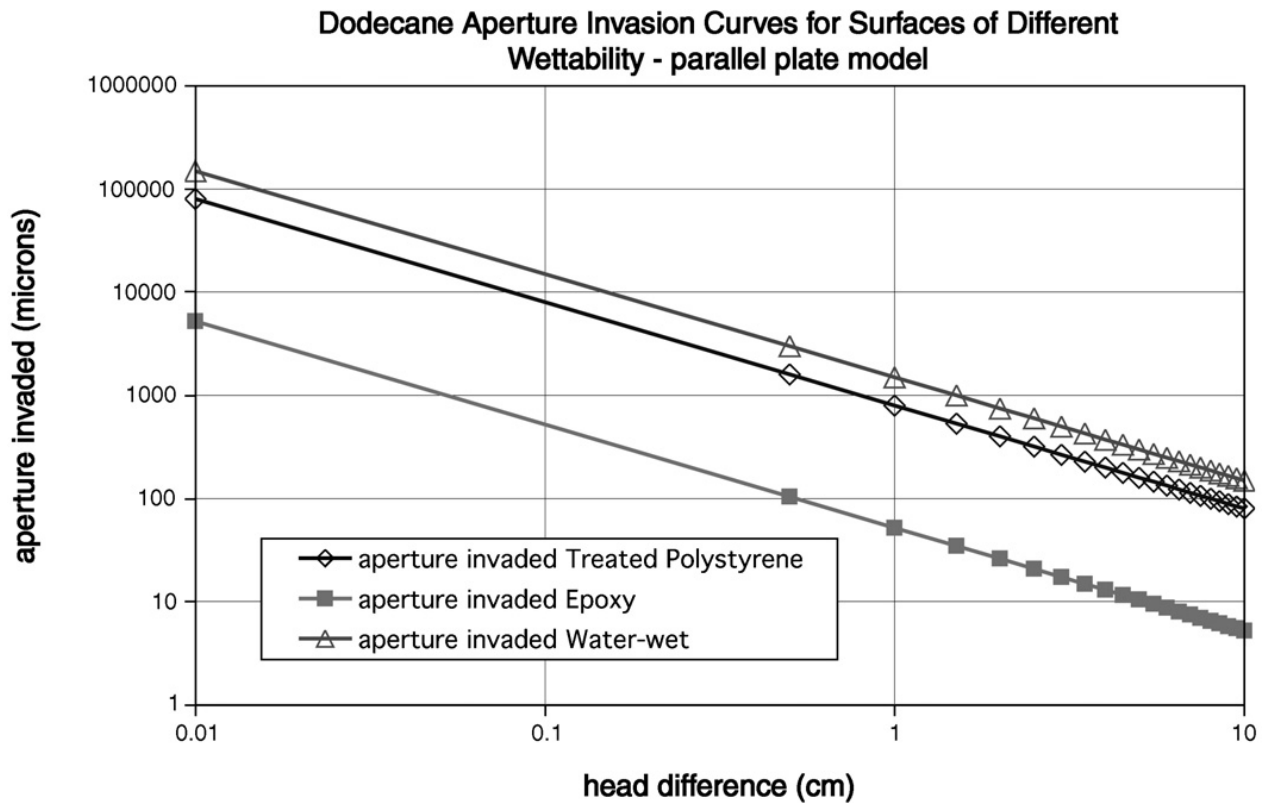


Fig. 17. Dodecane invasion curves for surfaces of differing wettability.

fracture replica, where invasion occurs spontaneously into even the smallest apertures (Fig. 18). While translucent epoxy models are useful tools for investigation of flow behavior in fractures, great care must be taken in interpretation of the results. They are not sufficiently good models to be used without careful selection of the immiscible fluid system, or to be used unquestioned as physical analogues for “natural rock.”

Theoretical invasion curves for various wetting conditions and non-wetting fluids can be calculated in a similar way (Fig. 19). Such curves can be used to determine if the model being utilized is a good analogue for the physical system under investigation or not.

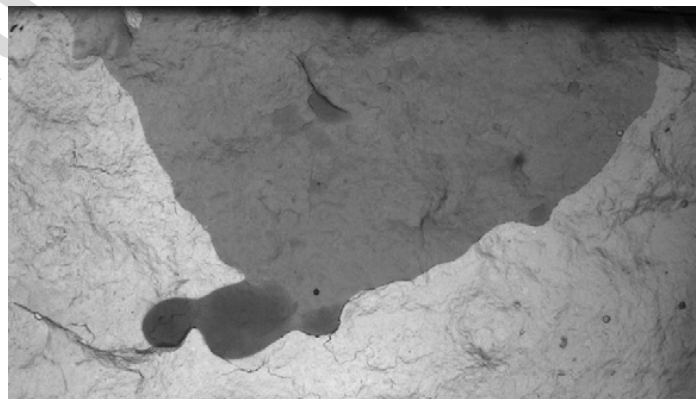


Fig. 18. Dodecane invasion of an epoxy fracture replica RN4.

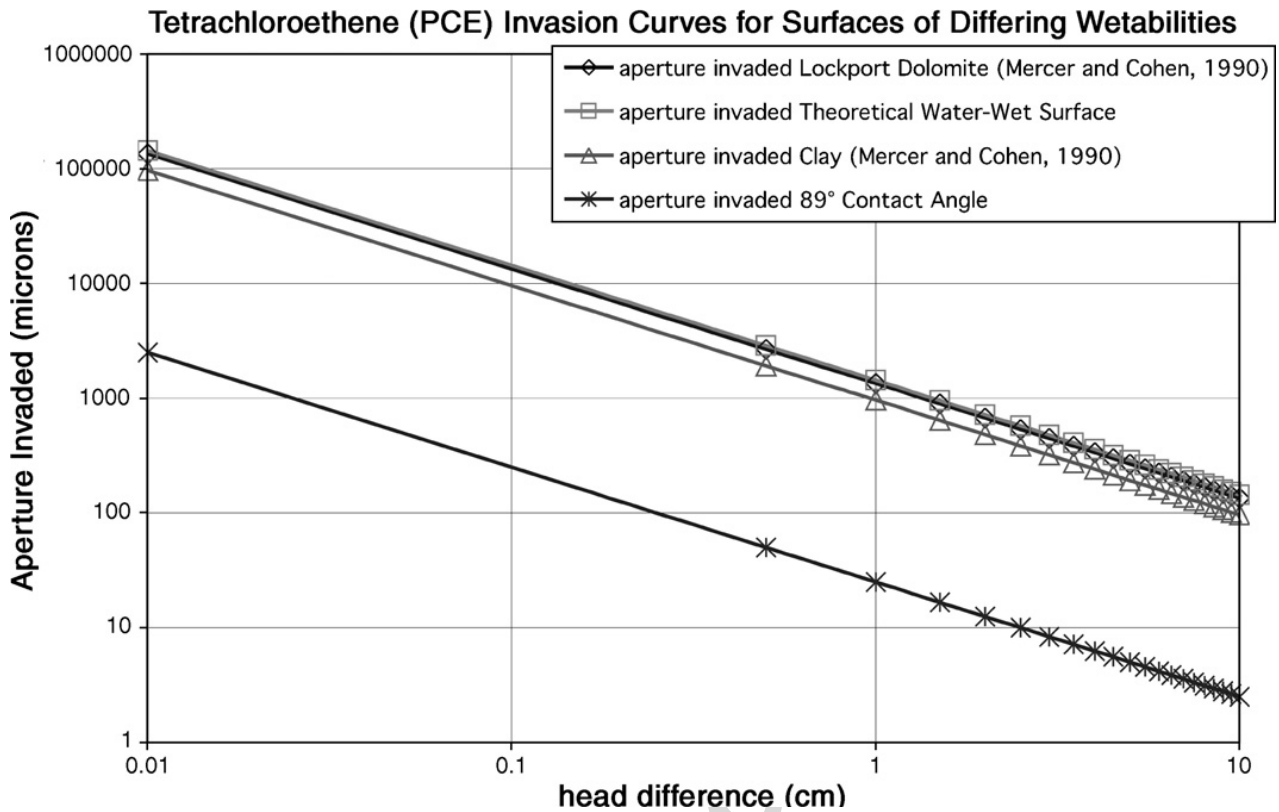


Fig. 19. Aperture invasion curves for PCE into surfaces of differing wettability.

Capillary pressure saturation curves are determined for the models by summing the total aperture of an invaded image, dividing that number by the sum of saturated apertures in a fully water saturated image and multiplying by one hundred (Fig. 20). Therefore, it appears that there is NAPL contact with the replica walls, or that there is some mechanism by which the interfacial tensions between the fluids and the solid is transmitted through thick layers of fluid.

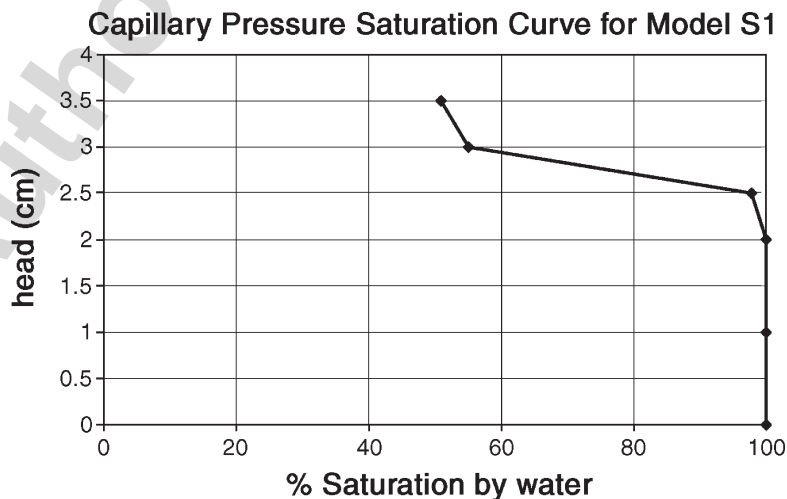


Fig. 20. Capillary pressure (cm of FC-75) versus saturation curve for model S1.

## 6. Conclusions

Two main questions were addressed in this study. First, are the commonly used epoxy replicas sufficiently accurate representations of natural fractures, and second, what are the effects of changes in wettability on NAPL flow and distribution in single fractures. Detailed characterization of the epoxy used for replica creation reveals that the epoxy is in fact slightly hydrophobic with a  $\gamma^-$  equal to 23.3 dyn/cm, where hydrophobic is defined as  $\gamma^-$  less than 28 dyn/cm (van Oss and Good, 1988; van Oss and Giese, 1995; Bergslien et al., 2004). This means that it is not a particularly good analogue for hydrophilic geologic media.

The more difficult question to answer is whether the effects of different wettabilities are of a significantly large degree to require changes in field investigation methods or computer model development. This work has demonstrated that changes in surface wettability can result in dramatically different flow behavior and residual distributions. For most cases, in hydrophobic replicas, like untreated polystyrene, the NAPL flows freely, displacing the water and filling virtually all of the pore space. In hydrophilic replicas, the NAPL is confined to the largest aperture pathways, resulting in isolated blobs with limited accessible surface area. The percentage of a fracture occupied by NAPL is significantly smaller in the hydrophilic models than in identical models with hydrophobic surfaces.

Certainly, the pulsing flow behavior and channel abandonment behaviors discussed previously are significantly different from those assumed in current modeling practice. The traditional modeling approach predicts that an immiscible invasive liquid will proceed with a spatially uniform invasion front and that, once an area is occupied, it will remain occupied until there is a new invasion of wetting fluid (Wang and Narasimhan, 1985; Peters and Klavetter, 1988; Nitao and Buscheck, 1991). The experiments in this study successfully show that neither of these assumptions is completely accurate. In addition, significant further research is called for on the actual saturation of apertures, the physical location of the NAPL and water within the void space, and the methods by which flow occurs without full occupation of the fracture void space. Development of models that successfully predict invasion behavior and distribution of NAPL in fracture networks will need to incorporate new ideas as to how NAPL flow occurs in fractures.

The key to determining whether surface wettability is negligible (i.e. the water-wet assumption holds) or not lies in characterization of the geologic media under study and with respect to the specific chemical system involved. Truly water-wet surfaces are rare (van Oss and Good, 1988). But, as long as the triple-point contact angle of the system under examination is low ( $<20^\circ$ ), the assumption of perfect water wettability is not a bad one (Fig. 19). The greater the triple-point contact angle, the more important and larger the effects of the surface chemistry on NAPL flow behavior and distribution. Casually assuming that all geologic material is water-wet is both inaccurate and potentially very misleading.

Currently, there is little detailed characterization of actual wetting behavior of natural geologic materials, and the effects of contact and aging of a NAPL on geologic media have been insufficiently explored (Powers et al., 1996; Seethepalli et al., 2004). By taking into account the problems and limitations discussed above, transparent fracture models are useful tools for exploration of a variety of issues, and with careful and considered use, provide a significant fund of experimental information.

## References

- 3M. Material Data Safety Sheet for Perfluoro-compound FC-75. 3M, 10 p.
- Adamson, A.W., 1990. *Physical Chemistry of Surfaces*. John Wiley and Sons. 777 pp.
- Bear, J., 1972. *Dynamics of Fluids in Porous Media*. Elsevier, New York, NY.

- Bergslien, E.T., Fountain, J.C., Giese Jr., R., 2004. Characterization of the surface properties of epoxy-type models used for multiphase flow studies in fractured media and creation of a new model. *Water Resour. Res.* 40 (5), W05112.
- Bradford, S.A., Leij, F.J., 1995. Wettability effects on scaling two- and three-fluid capillary pressure-saturation relations. *Environ. Sci. Technol.* 29, 1446–1455.
- Brett, C.E., Tepper, D.H., Goodman, W.M., LoDuca, S.T., Eckert, B., 1995. Revised stratigraphy and correlations of the Niagaran Provincial Series (Medina, Clinton, and Lockport Groups) in the type area of western New York. U.S. Geological Survey Bulletin, vol. 2086. 66 pp.
- Brown, Stephen R., Kranz, Robert L., Bonner, Brian P., 1986. Correlation between the surfaces of natural rock joints. *Geophys. Res. Lett.* 13 (13), 1430–1433.
- Brown, S., Caprihan, A., Hardy, R., 1998. Experimental observation of fluid flow channels in a single fracture. *J. Geophys. Res.* 103 (B3), 5125–5132.
- Corey, A.T., 1986. *Mechanics of Immiscible Fluids in Porous Media*. Water Resources Publications. 259 pp.
- Desmond, A.H., Desai, F.N., Hayes, K.F., 1994. Effect of cationic surfactants on organic liquid water capillary–pressure saturation relationships. *Water Resour. Res.* 30 (2), 333–342.
- Detwiler, R.L., Rajaram H., Glass R.J., 2005. Satiated relative permeability of variable-aperture fractures. *Physical Review E.* 71(3), 031114, 1–9.
- Dullien, F.A.L., 1992. *Porous Media: Fluid Transport and Pore Structure*. Academic Press, New York.
- Fisher Scientific, 1998. Material Data Safety Sheet for Perfluoro-compound FC-75. Fisher Scientific. 5 pp.
- Fourar M., 1992. Analyse expérimentale et modélisation des écoulements diphasiques en fracture, thèse de doctorat, Int. Natl. Polytech. de Toulouse, Toulouse, France.
- Fourar, M., Piquemal, J., Bories, S., 1991. Ecoulement diphasique bidimensionnel plan liquide-gaz: 2. Gradients de pression et fractions volumiques de phases d'un écoulement horizontal. *C. R. Acad. Sci., Ser. 2* 313 (2), 477–480.
- Fourar, M., Bories, S., Lenormand, R., Persoff, P., 1993. Two-phase flow in smooth and rough fractures: measurement and correlation by porous-medium pipe flow models. *Water Resour. Res.* 29 (11), 3699–3708.
- Geller, J.T., Su, G., Pruess, K., 1996. Preliminary Studies of Water Seepage Through Rough-walled Fractures, LBNL-38810, p. 73.
- Geller, J.T., Holman, H.Y., Su, G., Pruess, K., Hunter-Cevera, J.C., 2000. Flow dynamics and potential for biodegradation of organic contaminants in fractured rock vadose zone. *J. Contam. Hydrol.* 43, 63–90.
- Gentier, S., 1986. Morphologie et comportement hydromécanique d'une fracture naturelle dans un granite sous contrainte normale. Ph.D., Univ. d'Orleans, France.
- Gentier, S., Billaux, Van Vliet, L., 1989. Laboratory testing of the voids of a fracture. *Rock Mech.* 22, 149–157.
- Glass, R.J., Rajaram, H., Nicholl, M.J., Detwiler, R.L., 2001. The interaction of two fluid phases in fractured media. *Curr. Opin. Colloid Interface Sci.* 6, 223–235.
- Glass, R.J., Nicholl, M.J., Ramirez, A.L., Daily, W.D., 2002. Liquid phase structure within an unsaturated fracture network beneath a surface infiltration event: field experiment. *Water Resour. Res.* 38 (10), 1199. doi:10.1029/2001WR00167.
- Hakami, E., Barton, N., 1990. Aperture measurements and flow experiments using transparent replicas of rock joints. *Proceedings of the First International Symposium on Rock Joints*, pp. 383–390.
- Hakami, E., Larson, E., 1996. Aperture measurements and flow experiments on a single natural fracture. *Int. J. Rock Mech. Min. Sci. Geomech. Abstr.* 33 (4), 395–404.
- Jadhunandan, P.P., Marrow, N.R., 1995. Effect of wettability on waterflood recovery for crude-oil/brine/rock systems. *SPE Reserv. Eng.* 10 (1), 40–46.
- Kueper, B.H., 1989. The behavior of dense, non-aqueous phase liquid contaminants in heterogeneous porous media. Ph. D. Thesis, University at Waterloo, Ontario, Canada, 166 p.
- Kueper, B.H., McWhorter, D.B., 1991. The behavior of dense, nonaqueous phase liquids in fractured clay and rock. *Groundwater* 29 (5), 716–728.
- Kumar, A.T.A., Majors, P.D., Rossen, W.R., 1995. Measurement of aperture and multiphase flow in fractures using NMR imaging. *Proceedings of SPE Annual Technical Conference and Exhibition* SPE Paper, vol. 30558.
- Laroussi, C., DeBacker, L.W., 1979. Relations between geometrical properties of glass beads media and their main  $\psi(\theta)$  hysteresis loops. *Soil Sci. Soc. Am. J.* 43, 646–650.
- Lord, D.L., 1999. Influence of organic acid and base solution chemistry on interfacial and transport properties of mixed wastes in the subsurface. Ph.D. dissertation, Civil and Environmental Engineering, University of Michigan, Ann Arbor. 190 pp.
- Mendoza, C.A., 1992. Capillary pressure and relative transmissivity relationships describing two-phase flow through rough-walled fractures in geologic materials. Doctoral Thesis Department of Earth Sciences, University of Waterloo, Canada.
- Mercer, J.W., Cohen, R.M., 1990. A review of immiscible fluids in the subsurface. *J. Contam. Hydrol.* 6, 107–163.
- Merrill L.S., 1975. Two-phase flow in fractures. Ph.D., Univ. of Denver.

- Morrow, N.R., 1990. Wettability and its effect on oil recovery. *J. Pet. Technol.* 42 (12), 1476–1484.
- Morrow, N.R., Lim, H.T., Ward, J.S., 1986. Effect of crude-oil-induced wettability changes on oil recovery. *SPE Form. Eval.* 1 (2), 89–103.
- Nicholl, M.J., Glass, R.J., Wheatcraft, S.W., 1994. Gravity-driven infiltration instability in initially dry nonhorizontal fractures. *Water Resour. Res.* 30, 2533–2546.
- Nitao, J., Buscheck, T., 1991. Infiltration of a liquid front in an unsaturated, fractured porous medium. *Water Resour. Res.* 27 (8), 2099–2112.
- NRC, 1996. *Rock Fractures and Fluid Flow: Contemporary Understanding and Applications*. National Academy Press.
- Pankow, J.F., Cherry, J.A., 1998. *Dense Chlorinated Solvents and Other DNAPLs in Groundwater*. Waterloo Press, Portland, Oregon.
- Persoff, P., Pruess, K., 1993. Flow visualization and relative permeability measurements in rough-walled fractures. *Proceedings of the Fourth International High-Level Radioactive Waste Management Conference*. Las Vegas, Nevada, April 26–30, vol. 2. American Society of Civil Engineers, New York, pp. 2007–2019.
- Persoff, P., Pruess, K., 1995. Two-phase flow visualization and relative permeability measurement in natural rough walled fractures. *Water Resour. Res.* 31 (5), 1175–1186.
- Peters, R.R., Klavetter, E.A., 1988. A continuum model for water movement in an unsaturated fractured rock mass. *Water Resour. Res.* 24 (3), 416–430.
- Powers, S.E., Tamblin, M.E., 1995. Wettability of porous media after exposure to synthetic gasolines. *J. Contam. Hydrol.* 19 (2), 105–125.
- Powers, S.E., Anckner, W.H., Seacord, T.F., 1996. Wettability of NAPL-contaminated sands. *J. Environ. Eng.* 122 (10), 889–896.
- Pruess, K., Tsang, Y.W., 1990. On two-phase relative permeability and capillarity in rough-walled rock fractures. *Water Resour. Res.* 26 (9), 1915–1926.
- Pyrak-Nolte, L.J., Nolte, D.D., Myer, L.R., Cook, N.G.W., 1990. Fluid flow through single fractures. In: Barton, Stephansson (Eds.), *Rock Joints*. Balkema, Rotterdam, pp. 405–412.
- Pyrak-Nolte, L.J., Helgeson, D., Haley, G.M., Morris, J.W., 1992. Immiscible fluid flow in a fracture. *Proceedings, 33rd U.S. Rock Mechanics Symposium*, pp. 571–578.
- Reimus, P.W., Robinson, B.A., Glass, R.J., 1993. Aperture characteristics, saturated fluid flow, and tracer transport calculations for a natural fracture. *High-Level Radioactive Waste Management, Proceedings of the 4th Annual International Conference*. American Nuclear Society, LaGrange Park, IL, pp. 2009–2016.
- Reitsma, S., Kueper, B.H., 1994. Laboratory measurement of capillary pressure–saturation relationships in a rock fracture. *Water Resour. Res.* 30 (4), 865–878.
- Romm, E.S., 1966. *Fluid flow in fractured rock*. (in Russian) 283 pp. Nedra, Moscow, Russia. Translated by the Phillips Petroleum Company in 1972, 283 p.
- Seethapalli, A., Adibhatia, B., Mohanty, K.K., 2004. Physiochemical interactions during surfactant flooding of fractured carbonate reservoirs. *SPE J.* 9 (4), 411–418.
- Selker, J.S., Schroth, M.H., 1998. Evaluation of hydrodynamic scaling in porous media using finger dimensions. *Water Resour. Res.* 34 (8), 1935–1940.
- Schwille, F., 1988. *Dense Chlorinated Solvents in Porous and Fractured Media*. Lewis, Chelsea, Mich. 146 pp.
- Shapiro, A.M., Nicholas, J.R., 1989. Assessing the validity of the channel model of fracture aperture under field conditions. *Water Resour. Res.* 25, 817–828.
- Silpack Inc., 1996. *Silpack Inc. Technical Data Sheet*, Pamon, CA., Silpack Inc. 4 p.
- Steele, A., Lerner, D.N., 2001. Predictive modeling of NAPL injection tests in variable aperture spatially correlated fractures. *J. Contam. Hydrol.* 49 (3–4), 287–310.
- Su, G.W., 1995. *Water infiltration and intermittent flow in rough-walled fractures*. Masters Thesis, Dept. Civil Engineering, University of California, Berkeley.
- Su, G.W., Geller, J.T., Pruess, K., Wen, F., 1999. Experimental studies of water seepage and intermittent flow in unsaturated, rough walled fractures. *Water Resour. Res.* 35, 1019–1037.
- Su, G.W., Geller, J.T., Hunt, J.R., Pruess, K., 2004. Small-scale features of gravity-driven flow in unsaturated fractures. *Vadose Zone J.* 3 (2), 592–601.
- van Oss, C.J., Giese Jr., R.F., 1995. The hydrophilicity and hydrophobicity of clay minerals. *Clays Clay Miner.* 43 (4), 474–477.
- van Oss, C.J., Good, R.J., 1988. On the mechanism of “hydrophobic” interactions. *J. Dispers. Sci. Technol.* 9 (4), 355–362.
- Vickers, B.C., Neumann, S.P., Sully, M.J., Evans, D.D., 1992. Reconstruction and geostatistical analysis of multiscale fracture apertures in a large block of welded tuff. *Geophys. Res. Lett.* 19 (10), 1029–1032.

- Wang, J.S.Y., Narasimhan, T.N., 1985. Hydrologic mechanisms governing fluid flow in partially saturated, fractured porous medium. *Water Resour. Res.* 21 (12), 1861–1874.
- Wilson, J.R., Conrad, S.H., 1984. Is physical displacement of residual hydrocarbons a realistic possibility in aquifer restoration? *Proceedings of the NWWA/API Conference on Petroleum Hydrocarbons and Organic Chemicals in Ground Water*. National Water Well Assoc., Worthington, Ohio, pp. 274–298.

Author's personal copy